We are IntechOpen, the world's leading publisher of Open Access books
Built by scientists, for scientists

6,900
Open access books available

185,000
International authors and editors

200M
Downloads

154
Countries delivered to

Our authors are among the

TOP 1%
most cited scientists

12.2%
Contributors from top 500 universities

CLARIVATE ANALYTICS
BOOK CITATION INDEX
INDEXED

WEB OF SCIENCE™

Selection of our books indexed in the Book Citation Index
in Web of Science™ Core Collection (BKCI)

Interested in publishing with us?
Contact book.department@intechopen.com

Origins of the High Reactivity of Au Nanostructures Deduced from the Structure and Properties of Model Surfaces

Sandra Hoppe and Lyudmila V. Moskaleva

Additional information is available at the end of the chapter

Abstract

In this chapter, experimental and theoretical studies on surface segregation in Ag-Au systems, including our own thermodynamic studies and molecular dynamics simulations of surface restructuring, on the basis of density functional theory are reviewed. The restructuring processes are triggered by adsorbed atomic O, which is supplied and consumed during catalysis. Experimental evidence points to the essential role of Ag impurities in nanoporous gold for activating O_2. At the same time, increasing Ag concentration may be detrimental for the selectivity of partial oxidation. Understanding the role of silver requires a knowledge on its chemical state and distribution in the material. Recent studies using electron microscopy and photoelectron spectroscopy shed new light on this issue revealing a non-uniform distribution of residual Ag and co-existence of different chemical forms of Ag. We conclude by presenting an outlook on electromechanical coupling at Ag-Au surfaces, which shows a way to systematically tune the catalytic activity of bimetallic surfaces.

Keywords: nanoporous gold, Au-Ag alloy, surface, segregation, atomistic simulations, cluster expansion, density functional theory, electromechanical coupling, ab initio

1. Introduction

For centuries, the use of gold has been restricted mainly to jewelry and coinage. Being considered unreactive, gold did not represent an attractive material for catalytic applications [1]. This image began to change in the 1970s, when the first studies hinted at the potential reactivity of small gold particles [2–5]. In 1985, Hutchings reported that cationic gold was the best catalyst

for hydrochlorination of acetylene to vinyl chloride [6]. At about the same time, Haruta et al. [7, 8] discovered the high reactivity of ultra-fine Au particles supported on 3d transition metals as a catalyst for aerobic CO oxidation at temperatures below 0°C. Not only gold's reactivity caught the attention of the catalytic community, but also its selectivity, as it has been found that gold does not attack C–C or C–H bonds in organic compounds [9]. These characteristics make gold a promising candidate for "green chemical industry," especially for developing processes operating at ambient pressure and temperature with the benefit of avoiding toxic materials [10]. More recent studies focused on bimetallic Ag-Au nanoparticles supported on aluminosilicate [11–14] or titania [15] for low temperature CO oxidation. Compared to monometallic Au nanoparticle catalysts, they showed higher catalytic activity [11–14, 16, 17].

Through electrochemical corrosion and selective leaching of the second metal (typically silver) from a bimetallic Au-M (M = Ag, Cu, Al, Si) alloy, the sponge-like nanoporous gold (npAu) can be obtained [18–20]. The microstructure and ligament dimensions of this unsupported catalyst can be adjusted in its synthesis as desired for the respective application. Its open porosity makes it permeable for liquids as well as gases. Furthermore, it possesses a strongly curved surface with a very high surface-to-volume ratio [18, 19]. Research on npAu has mainly focused on aerobic CO oxidation [19, 21–26] and oxidative coupling/cross-coupling of alcohols [8, 22, 26]. The partial oxidation products, esters, are valuable bulk chemicals in chemical industry. In particular, methyl formate is formed in the oxidative coupling of methanol and provides an important precursor for the production of formic acid, formamide, and dimethylformamide [27]. Other organic transformations have also been explored as covered in recent reviews [26, 28–30].

The literature reports two possible origins for the high reactivity of npAu, for example, towards CO oxidation. First, the curved surface of the npAu ligaments shows high density of low-coordinated Au atoms at steps and kinks [31], which may serve as reactive sites. However, several studies dealing with oxygen adsorption on Au surfaces indicated that roughening the Au surfaces by sputtering did not make them active towards CO oxidation, unless atomic oxygen was pre-adsorbed at the surface, even though many low-coordinated Au atoms were present [32–35]. Second, the residual silver which is left in the npAu after the dealloying process was suggested to promote reactivity [21, 36, 37]. This has been proposed by Bäumer and associates [21, 37], who investigated the morphology, surface composition, and catalytic activity of npAu towards CO oxidation. Even for npAu samples with almost no Ag left in the bulk, Ag surface concentrations of up to 10% were measured. Importantly, all samples had to be activated for a certain time before catalytic activity was detected. While the morphology of the activated samples did not undergo any notable change during the activation, in situ X-ray photoelectron spectroscopy (XPS) characterization revealed a change in the chemical state of the Ag atoms at the surface. However, the chemical state of Ag was not clearly assigned. It could not be attributed to chemisorbed O on Ag or to Ag_2O or to AgO species. It was suggested [21, 37] that Ag impurities play a decisive role for the activation of molecular oxygen and that npAu should actually be considered a bimetallic catalyst.

The favorable role of Ag impurities for CO oxidation was corroborated in further experimental studies [25, 38], which demonstrated a clearly positive correlation between the Ag content in

the npAu samples and the catalytic activity. With the help of density functional theory (DFT) calculations and using the stepped and kinked Au (321) model surface to mimic the structural motifs of npAu, Moskaleva et al. [39] found an increase in the adsorption strength of O_2 and a reduction of the O_2 dissociation barrier with the increasing size of Ag ensembles at the reaction site located at the step edge. These Ag ensembles were identified as sites capable to dissociate O_2 and to supply atomic O to surrounding Au sites, where it may then react with chemisorbed CO to form CO_2. Consequently, a high density of atomic steps at the ligament surface as well as the presence of surface Ag impurities is believed important for achieving high catalytic activity.

Fujita et al. [31] established a connection between the rough npAu surface and the residual Ag content via *in situ* high-resolution TEM of npAu catalyzing CO oxidation. They reported that a higher residual Ag content suppressed {111} faceting at the surface and thereby stabilized steps and kinks containing many low-coordinated Au atoms. Hence, the role played by Ag for the high catalytic activity of npAu appears to be twofold and consists of the supply of reactive sites on the one hand and of the preservation of the rough morphology on the other hand.

Within our studies reviewed in this chapter, we shed new light on the distribution of Ag in Ag-Au surfaces and on the role of Ag for the reactivity of npAu. To this end, we first analyzed the segregation behavior at the flat Ag-Au (111) surface to better understand the underlying phenomenology. Furthermore, we considered the effect of adsorbed oxygen on the surface composition. Apart from flat surfaces, we also studied silver segregation at the stepped Au (321) surface induced by adsorbed O atoms, the formation of –(Au-O)– oxide chains, and how such chains affect Ag segregation [40, 41]. In the following, we give an overview of experimental and theoretical studies on segregation in the Ag-Au system, followed by our theoretical results, directed at understanding segregation phenomena in npAu. Next, we reflect on the role of Ag impurities and Ag distribution at the catalyst surface for the catalytic activity. Finally, we give an outlook on ongoing investigations about electromechanical coupling at Ag-Au surfaces.

2. Surface segregation and restructuring

The term surface segregation refers to the concentration gradient at the surface of a material consisting of at least two elements resulting from diffusion of one component to the surface. This process is driven by a difference in chemical potential between the bulk and the surface and it may lead to a completely different atomic ordering and composition in the surface region compared to the bulk structure. Understanding segregation and surface reconstruction is important for many technologies involving heterogeneous catalysis, corrosion resistance, adsorption, or magnetic, electronic, and optical materials [42, 43], since these effects alter the physical and chemical properties at the surface. Consequently, various theoretical models to predict surface segregation based on different parameters have been developed over the last decades [44–48].

When a surface is created, bonds between atoms are locally broken, which is accompanied by a cost in energy. Within the framework of the so-called bond-breaking models, the total energy of the crystal is represented as the sum of pair-bond energies. Either an ideal (no enthalpy of mixing) or a regular (non-zero mixing enthalpy allowed) solution model can be adapted and depending on the choice of parameters, the resulting segregation may be limited to the surface layer only or include multiple layers. According to this theory, the element with the lowest bond strength will preferably be located at the surface to keep the energy cost as low as possible. To link this prediction to an experimentally measurable surface parameter, a correlation between the free energy of segregation and the surface energy has been established, yielding the surface segregation of the element with the lower surface energy [46]. Apart from different bond strengths, a potential atomic size mismatch may also affect the segregation behavior. If the element with the larger atomic radius is located at the surface, fewer atoms are needed to populate the surface layer and the number of broken bonds there is thus minimized. This approach consequently predicts segregation of the larger atomic species to the surface. An atomic size mismatch between two elements also leads to elastic strain contributions to the free energy of a material, because a solute atom residing in a significantly smaller or larger host lattice is surrounded by an elastic strain field. Within this model of continuum elastic theory, segregation of this solute atom to the surface would result in a relief of lattice strain in the bulk and is thus energetically favorable [46, 47, 49–51].

These two concepts involving broken bonds at the surface and elastic strain in the bulk may lead to contradicting results when applied separately [49], which is why they have been combined to achieve a more realistic prediction of surface segregation. Using pair-potential approximation models, for example, the total energy of a material is calculated as the sum of pairwise interactions. In contrast to the bond-breaking theory, however, relaxation of the atoms to their equilibrium positions is included, thereby also considering strain energy.

When applied to the Ag-Au system, which is of interest in this study, the theories described above result in a clear tendency: The strain contributions due to atomic mismatch should be negligible, since Ag and Au have almost the same lattice constant, with Au being slightly smaller [52]. If there was any size effect, it would cause Ag to sit in the surface layer to reduce the number of broken bonds. Additionally, Ag possesses a smaller surface energy than Au [53], which should also stabilize it in the topmost layer. Despite the seemingly clear answer coming from phenomenological theories, various experimental studies on surface segregation in the Ag-Au system from the past report conflicting results. Even if there is qualitative agreement between several papers, a quantitative agreement is hardly found in the literature. These conflicting results from the past may have their origin in either the choice of the experimental method, the calibration of instruments, or the sample preparation.

Thorough surface preparation represents a crucial procedure and also a major challenge for experiments targeting surface segregation. The desired surface orientation must be carefully cut and cleaned from contaminants, such as oxygen, carbon monoxide, and other gases, which may severely influence the segregation profile. In their review on the surface segregation in gold-containing alloys, Dowben et al. [51] stated that gold alloys are usually more easily characterized and yield more reliable results than other materials. They attribute this to a

simple cleaning procedure and a low contamination level on gold alloy surfaces due to low sticking coefficients of typical contaminants. Typical contaminants for the Ag-Au surface have been identified as S, Cl, O and N [54, 55]. They are commonly removed by successive Ar$^+$ sputtering and annealing procedures [51]. Regarding gold alloy surfaces, Dowben et al. [51] emphasize that preferential sputtering represents a usual problem and lengthy and thorough annealing steps are crucial to obtain surfaces in thermodynamic equilibrium.

Not only the way the samples are prepared but also the measurement techniques and even their respective calibration methods may influence the obtained results. This has been pointed out by Bouwman et al. [56], who conducted Auger Electron Spectroscopy (AES) measurements on annealed polycrystalline Ag-Au bulk samples with varying Ag content. In contrast to calculations employing the regular solution model, which predicts Ag enrichment in the surface layer, they observed a bulk-like surface composition, independent of temperature. While their results are in good agreement with an earlier AES study by Fain and McDavid [57] on epitaxially grown Ag-Au thin films, they stand in contrast to yet another AES study by Somorjai and Overbury [58], who reported Ag surface enrichment in polycrystalline Ag-Au foils. Bouwman et al. report that they applied a so-called "internal calibration," meaning they recorded AES spectra of the freshly cut, homogeneous Ag-Au surface as a reference. Somorjai and Overbury, however, recorded spectra from the respective elements, which is referred to as "external calibration." This example already illustrates possible difficulties in measuring surface segregation. Other possible source of incorrect data interpretation could be neglecting the effect of different backscattering factors of Ag and Au as pointed out by Overbury and Somorjai [54]. These authors reported slight Ag enrichment, which is, however, within the experimental error. They furthermore observed that cleaning the surface with Ag$^+$ led to Au surface enrichment. Similar observations were reported by Yabumoto et al. [55] for polycrystalline Ag-Au surfaces.

In experiments targeting surface segregation, it is of course desired to measure the composition of the very topmost layer and not only an averaged value over a certain number of atomic surface layers. Nelson [59] hinted at potential drawbacks of AES, including the uncertainty about backscattering contributions and as well the necessity to know the exact escape depth of the Auger electrons to evaluate the surface sensitivity of this method. He argued that ion scattering spectroscopy (ISS) represented a more suitable method to investigate surface segregation, as it offered monolayer sensitivity as well as the possibility to clean and anneal the sample *in situ*. His results for thoroughly polished polycrystalline Ag-Au samples indicated Ag surface enrichment, though slightly less pronounced than predicted by the regular solution model. Shortly afterwards, his findings were corroborated by an ISS study by Kelley et al. [60], who also reported Ag surface segregation in the Ag-Au system.

The AES and ISS studies summarized above have been carried out with polycrystalline samples, so that no conclusions could be drawn from them regarding the effect of crystallographic orientation for the segregation. King and Dononelly [61] addressed this issue by identifying (111), (110) and (100) planes on some surface domains or grains on their polycrystalline samples, applying low energy electron diffraction (LEED) and selected area channeling pattern (SACP). They used AES to obtain the composition of the first two surface layers for varying

crystallographic orientation, temperature, and Ag bulk concentration. In agreement with Monte Carlo simulations also conducted in their work, King and Dononelly found strong Ag surface segregation for the Ag-Au (100) domains, while it is less pronounced for the (110) domains and relatively weak for the (111) planes. Shortly afterwards, Meinel et al. [62] investigated epitaxially grown Ag-Au films with (111) orientation via AES. Even though they also found Ag surface enrichment, their results did not agree quantitively with those from King and Dononelly, but rather with the ISS results from Nelson [59] and Kelley [60].

The first surface structural measurement on a Ag-Au surface was conducted by Derry and Wan [63], who performed a LEED structure analysis of the Ag-Au (100) surface of an alloy containing 50% Ag. Derry and Wan predicted Ag enrichment in the surface layer and slight Ag depletion in the subsurface layer, but no quantitative agreement with earlier studies was reached.

In summary, experimental results on surface segregation in the Ag-Au system reach from no observed segregation to very pronounced Ag surface enrichment, but there is no quantitative consistency. As mentioned before, this may arise due to different measurement techniques, choice of parameters and calibration methods, and different sample characteristics.

A wide variety of simulation methods available today represents a promising way to verify or explain the experimental outcomes of segregation studies. However, theoretical studies on the surface segregation at Ag-Au extended surfaces are relatively scarce. Bozzolo et al. [64] studied segregation behavior in Ag-Au. In their quantum approximate approach, the energy of a certain atomic configuration is calculated as the sum of strain energy and chemical atomic contributions. The parameters required for their simulations were determined from first principles LAPW calculations. While their simulations yielded Ag enrichment in the surface layer and Ag depletion in the subsurface layer in all cases, they found a strong dependence of the amount of segregation on temperature and Ag bulk concentration. Interestingly, for the $Ag_{30}Au_{70}$ (100) surface, they obtained a perfectly ordered surface layer and a pure Au subsurface layer for temperatures approaching 0 K. At about 100 K, a drastic change in segregation behavior occurred and the surface plane was pure Ag. From there on, the Ag surface layer concentration decreased monotonically until reaching an approximately constant value around 600 K. The authors attribute this phenomenon to two competing effects: the favorable Ag–Au bonds lead to ordering at low temperatures and the lower surface energy of Ag causes it to segregate to the surface at higher temperatures.

Since nanoparticles are highly interesting for the catalytic community, many studies focusing on the structure and composition of Ag-Au clusters of various sizes can be found in the literature. Conflicting results emerged from these theoretical works, depending on the simulation method and choice of input parameters. In a Monte Carlo study on the segregation in trimetallic Ag-Cu-Au clusters, Cheng et al. [65] predicted Ag segregation to the surface of the particles, while Cu was located at the center and Au mainly in the middle shell. As Cu possesses the highest surface energy, followed by Au and then Ag, their results are in good agreement with simple bond-breaking models.

Curley et al. [66] simulated bimetallic Ag-Au clusters containing 38 atoms with an empirical potential, the so-called "Gupta potential," based on tight-binding theory and combined it with

a genetic-algorithm search technique to identify energetically favorable compositions. In these favorable structures, they found a clear Ag enrichment in the particle surface and explained their findings by the lower surface energy of Ag and the strong Au–Au metal bonds, stabilizing Au in the core of the particle. In their discussions, they argue that an electron transfer from the less electronegative Ag to Au should promote heterometallic Ag–Au bonds. However, according to them, the fact that Ag-Au is a random alloy without order may speak for a negligible effect of charge transfer.

In Monte Carlo simulations based on the modified analytic embedded atom method (MAEAM), Deng et al. [67] predicted segregation in Ag-Au nanoparticles and analyzed the effect of composition, particle size, and temperature. A more pronounced Ag surface enrichment was obtained for a higher Ag bulk concentration, larger particles, and lower temperature. They furthermore mention a possible influence of a charge transfer from Ag to Au, but state that this influence was small for large particles and bulk materials. Indeed, numerous studies found this charge transfer to promote heterometallic Ag–Au bonds and to stabilize Au in the shell of small Ag-Au particles containing less than eight until up to 20 atoms [68–72]. It is worth noting that almost all these studies employed density functional theory (DFT) calculations, while most of the investigations of larger particles were carried out with empirical potentials [67, 73].

In this context, Paz-Borbon et al. [73] made an interesting observation when they studied the segregation behavior of 38-atom binary clusters composed of transition metals. They used an empirical Gupta potential combined with a genetic algorithm to identify energetically favorable structures, which were then investigated further via DFT calculations. To analyze the correct chemical order, they also inverted the positions of the respective elements in clusters containing 19 atoms of each species. Like in previous studies employing empirical potentials, the Gupta potential yielded Ag segregation to the surface of the particle, while Au was located at the core. Surprisingly, DFT optimization and calculation of the inverted particle resulted in the contrary, namely that a particle with a Au shell and Ag core was energetically most favorable. While models considering surface energies and bonding interactions would not predict Au surface segregation, Paz-Borbon et al. [73] explained this discrepancy with a charging effect from Ag to the more electronegative Au, which is not captured by standard empirical potentials. As their calculations were limited to 38 atom nanoparticles, it is, of course, questionable, whether their findings can be transferred to clean Ag-Au surfaces. There exists, however, a DFT study by Dianat et al. [74] revealing the influence of charge transfer on the segregation at the adsorbate-free and oxygen-covered Pt-Pd surface. Their work was motivated by a discrepancy between experimental results observing a Pt-enriched surface and simulations using the embedded atom model or empirical potentials, which indicated Pd surface segregation. The segregation behavior they obtained for the Pt-Pd (111) surface modeled in a 1×1 cell depended on the underlying bulk composition. For a Pd-rich bulk, Pd was preferably located at the surface, as the element with the lower surface energy. For a Pt-rich bulk, however, the energetically most favorable configuration had a Pt surface and a Pd subsurface layer. With the help of a Bader analysis [75–78], they showed that for all surface structures, a charge transfer from Pd to the more electronegative Pt takes place. Thereby, the d-band filling of the surface Pt atoms is increased, while the d-bands of the subsurface Pd atoms

are depleted. Dianat et al. [74] argued that according to a model proposed by Friedel et al. [79], the surface energy of metals with more than half-filled *d*-bands decreased upon increasing *d*-band filling. Therefore, the calculated charge transfer stabilizes Pt at the surface, even though it has the higher surface energy. Upon oxygen adsorption, the strong affinity of Pd towards O caused Pd segregation to the surface layer in all calculated structures.

Thus, the charge transfer caused by the difference in electronegativity between Pt and Pd is a decisive factor for segregation. The electronegativity values on the Pauling scale amount to 2.28 and 2.20 for Pt and Pd, respectively, and to 2.54 and 1.93 for Au and Ag, respectively. This larger difference theoretically implies an even larger charge transfer between Ag and Au. In our investigations on surface segregation at Ag-Au surfaces [39, 79] reviewed below, we aimed at shedding light on the subtle mechanisms leading to the energetically most favorable surface configurations. As those mechanisms may be captured by accurate quantum mechanical modeling, we employed DFT calculations in combination with statistical physics to scan the whole configuration space. An overview of the methods we applied will be given in the next section.

3. Methodology

In this section, we will give an overview of the methods applied in our study on segregation, dynamic restructuring, and electromechanical coupling at Ag-Au surfaces. A more detailed report of important calculation parameters and information on the surface models is given in Refs. [40, 41, 80].

3.1. Density functional theory calculations

The modeling studies reviewed in the following have been performed on the basis of density functional theory (DFT) [81]. In the past two to three decades, DFT has developed into a powerful methodology. Thanks to the computational power available nowadays, electronic structure calculations of systems containing hundreds of atoms can be handled, making DFT-based approaches attractive for material science, computational physics, and chemistry.

Static DFT calculations reported below were carried out with the program code Vienna ab initio simulation package (VASP) [82–85], employing plane-wave basis sets to expand the electron density. Ab initio molecular dynamics (AIMD) simulations of surface restructuring were carried out with the CP2K software [86], which uses mixed plane-wave and Gaussian basis sets. Concerning the choice of an appropriate exchange-correlation functional, we had several prerequisites. As already mentioned in Section 2, two critical quantities, which may influence the segregation behavior, are the surface energy and the equilibrium lattice parameter. To ensure as realistic predictions of the segregation behavior at Ag-Au surfaces as possible, we aimed at fulfilling two conditions observed experimentally: First, the two lattice constants of the pure elements should be almost identical and second, silver should have a smaller surface energy than gold. We found reasonable agreement with experimental values for the

GGA Perdew-Burke-Ernzerhof functional (PBE) [87, 88] with additional dispersion corrections (DFT-D3) as proposed by Grimme et al. [89]. In this approach, the total energy equals the sum of the energy resulting from electronic convergence with PBE plus a van der Waals correction term which is added subsequently. This functional was thus employed in all DFT calculations to investigate surface segregation. The AIMD simulations were carried out using PBE functional, without including dispersion corrections, because the qualitative trends were not affected by including D3 correction, as test calculations have revealed. Our computational approach was based on periodic DFT and employed slab models. As one of our goals was to study the influence of Ag bulk concentration on the segregation profile, we considered three different clean (i.e. adsorbate-free) surfaces: cut from: pure Au bulk, pure Ag bulk, and from a L1$_2$ ordered bulk structure with 25% Ag, respectively. The latter was chosen as it represents a ground state in the Ag-Au phase diagram at very low temperatures. Additionally, an oxygen-covered surface slab cut from L1$_2$ bulk with O atoms occupying fcc hollow sites was built. In the (2 × 2) unit cell, this corresponds to O coverage of 0.25 monolayer (ML). Side and top views of the adsorbate-free and oxygen-covered surface slabs are shown in **Figure 1**.

Additionally, we modeled the stepped Au (321) surface with an infinite oxide chain. Such chains of alternating Au and O atoms were previously identified as a common feature of thermodynamically stable surface configurations of the Au (111) [90, 91], the Au (110) [92, 93] as well as the Au (321) [94] surfaces. The latter surface features steps and terraces with both high- and low-coordinated Au atoms and therefore provides an ideal model for the rough npAu surface morphology [31, 94, 95]. As this oxide chain structure was apparently stabilized by the presence of Ag with respect to the adsorbate-free surface [94], we aimed at finding the preferred atomic positions of Ag impurities within the oxygen-covered Au (321) surface. The asymmetric (2 × 1) surface slab contained 28 Au atoms and two O atoms (see **Figure 2**). This corresponds to an O coverage of 0.2 ML, which is the minimum possible coverage allowing for chain formation for the chosen unit cell size [94]. The lower 14 Au atoms were considered as
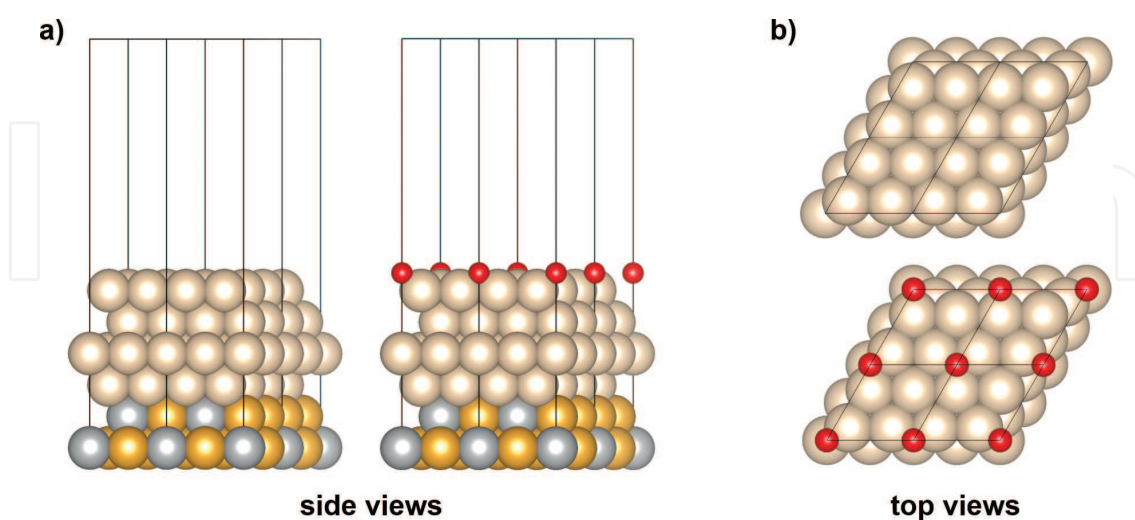

Figure 1. Side (a) and top (b) views of the adsorbate-free and oxygen-covered Ag-Au (111) surface slab with L1$_2$ bulk ordering. Au atoms are shown in yellow, Ag in gray, and O in red. The top four surface layers were allowed to be replaced by Au or Ag in the CE calculations and are depicted in beige. The (2 × 2) unit cell is indicated. Reproduced from Ref. [149] with the permission of AIP Publishing.
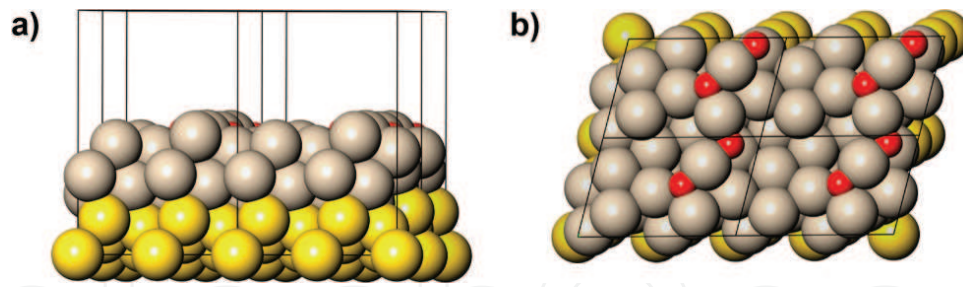
Figure 2. Side view (a) and top view (b) of the Au (321) surface slab with an infinite oxide chain. Atoms which were subsequently substituted by Ag are depicted in beige, while the O atoms are shown in red. The (2 × 1) unit cell is indicated. Reproduced from Ref. [40] with permission from the PCCP owner societies.

bulk atoms and kept fixed during the calculations, while the upper 14 Au atoms were allowed to relax. Since the DFT calculations served as input for the cluster expansion, the Ag content within the beige atoms in **Figures 1** and **2** was varied from 0 to 100%, with 0% corresponding to pure gold and 100% corresponding to all beige atoms occupied by silver.

3.2. Ab initio MD simulations

AIMD simulations based on DFT (at the GGA-PBE level) were performed at 700 K using the CP2K code [86]. We employed a (3 × 2) unit cell of the Au (321) surface. All initial geometries that served as input for AIMD simulations were fully optimized to a local minimum by means of electronic structure computations performed with CP2K. In the simulations, we used Nose-Hoover thermostat (NVT) to sample from the canonical ensemble [96, 97]. See Refs. [40, 41] for further details.

3.3. Cluster expansion and Monte Carlo simulations

Because calculating all possible surface configurations by means of DFT would represent a tedious, very time-consuming task, we tackled this problem by performing a cluster expansion (CE) [98], providing us access to the whole configuration space. Within the cluster expansion approach, the many-body interactions of a crystal structure are decomposed into a sum over bonds, also called figures or clusters. Any observable, which is a functional of the atomic configuration of all lattice points, can then be represented as a linear combination of characteristic interactions J_F of those clusters. Hence, the surface formation enthalpy $\Delta H_f^{surf}(\sigma)$ of structure σ with the two constituents A and B can be calculated as follows:

$$\Delta H_f^{surf}(\sigma) = \sum_F J_F \Pi_F(\sigma) - x_A^{surf}(\sigma) E_A^{slab} - x_B^{surf}(\sigma) E_B^{slab}, \tag{1}$$

where $\Pi_F(\sigma)$ is a correlation functional for each class of symmetry-equivalent clusters F, where equivalence is determined by the symmetry of the underlying grid of atomic sites. x_A^{surf} and x_B^{surf} are the respective concentration of the elements A and B within the atoms depicted in beige in **Figures 1** and **2**. The reference energies of surfaces with only Au or Ag at these positions are given by E_A^{slab} and E_B^{slab}, respectively. Throughout our work, we used the program

package UNCLE [99] to perform the surface cluster expansions. Starting from a random set of DFT input structures, each of which contained the unrelaxed atomic coordinates with the corresponding total energy of the fully relaxed geometry, the values of J_F were determined via a genetic algorithm [100, 101]. In a next step, energetically favorable surface configurations were identified on the basis of the obtained Hamiltonian and employing an exhaustive enumeration algorithm [101–103]. These structures were then calculated at the DFT level and added to the input database, thereby iteratively improving the fit quality regarding configurations close to the convex hull of the energetically most favorable structures, the so-called "ground-state line." When the predicted and the input ground state lines finally coincide, the cluster expansion is considered converged. The Hamiltonian resulting from the CE fit was subsequently employed in Monte Carlo simulations to account for the influence of configuration entropy on the surface segregation profile at higher temperatures. We thereby modeled a simulated annealing process for the clean as well as the partially oxygen-covered Ag-Au (111) surface cut from an L1$_2$-ordered bulk structure.

4. Computational studies of segregation on clean and O-covered Au-Ag surfaces

4.1. Segregation at the Ag-Au (111) surface

In a recent publication [80], we have analyzed the segregation behavior at the Ag-Au (111) surface. From the cluster expansion, we obtained surface formation enthalpies for all possible Ag concentrations and configurations within the four surface layers depicted in **Figure 1**. This allowed us to identify the energetically most favorable structures, the ground states, and to construct the convex hull curve [80]. Three exemplary ground states for the (111) surface with L1$_2$-ordered bulk are shown in **Figure 3** in top and side views, along with their corresponding Ag surface concentration x_{Ag}^{surf}. Interestingly, the CE predicts Au enrichment within the topmost surface layer, while the second topmost layer is enriched in Ag. For only one Ag atom
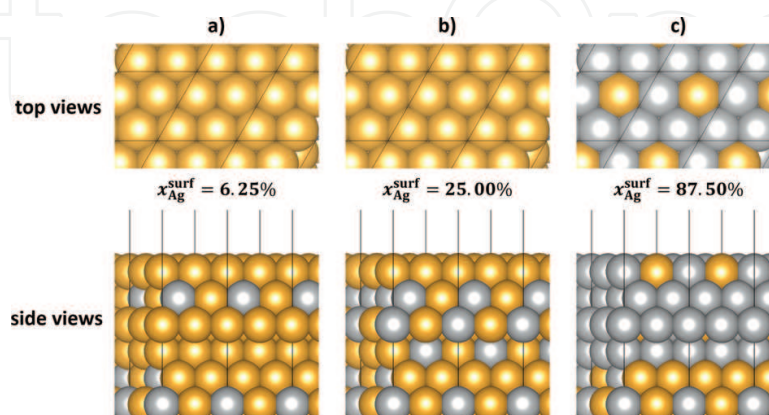

Figure 3. (a)–(c) Top and side views of three selected ground state surface configurations for the Ag-Au (111) surface with L1$_2$-ordered bulk. The respective Ag surface concentration x_{Ag}^{surf} is given below the top view.

replacing an Au atom within the four surface layers, the energetically preferred position is in the second topmost layer (see **Figure 3a**). With rising Ag surface concentration, the third and fourth layers adapt the L1$_2$ bulk structure, which agrees well with the tendency of Ag and Au to mix and form ordered structures close to 0 K and a solid solution at finite temperatures. Up to Ag surface concentrations of $x_{Ag}^{surf} = 31.25$ at.%, the topmost layer contains only Au atoms. Even for only one Au atom left within the four surface layers, that Au atom is located in the topmost layer for the energetically most favorable structure.

Our investigation showed that this segregation behavior is almost independent of the Ag bulk content, as the ground state surface configurations were nearly identical for pure Au bulk, pure Ag bulk, and the L1$_2$ bulk structure. To ensure that the obtained segregation profiles did not result from our choice of exchange-correlation functional, we repeated the CE with DFT input calculations employing different functionals: LDA, PBE, PBEsol, and opt86B-vdW. However, all functionals led to Au enrichment in the topmost layer. Even though the calculated surface formation enthalpies are fairly small, with values up to and around 35 meV, some driving force apparently causes Au to segregate to the topmost layer against predictions based on the surface energy hierarchies or lattice constants. As reported in Section 2, so far, no Au surface segregation has been observed experimentally for the Ag-Au system.

Comparing our results to those obtained for Pd-Pt by Dianat et al. [74], we believe that an electron transfer from Ag to Au caused by their large difference in electronegativity (1.93 and 2.54, respectively) stabilizes Au within the topmost surface layer. According to a model proposed by Friedel [79], further filling the d shell of a transition metal with an originally more than half-filled d shell leads to a decrease in surface energy. While this argument is plausible for Pd-Pt, both Ag and Au have filled 5d orbitals. Nevertheless, Au shows strong s-d hybridization, which decreases the energy gap between the 5d states and the 6s states and causes a depletion of the 5d states population. Hence, a charge transfer from Ag into the destabilized Au 5d orbital becomes possible. Our calculations comprising Bader analyses corroborate our assumption and show that a pure Au topmost layer followed by a pure Ag layer leads to a negative excess charge within the Au layer of -0.10 e (where e corresponds to the elementary charge). All ground states found for the CE for the (111) surface with L1$_2$ bulk have nearly the same excess charge within their topmost layer of about -0.04 e. Their configurations appear to be the result of the counteracting effects of charge transfer, the lower surface energy of Ag, and the general tendency of Ag and Au to mix and form heterometallic bonds.

The presence of adsorbed oxygen on an fcc hollow site, however, revokes this fine balance of interacting effects. The strong affinity of Ag towards oxygen causes the segregation behavior to reverse and draws Ag to the topmost surface layer. Our CE for the oxygen-covered (111) surface predicts that already for a Ag surface concentration of $x_{Ag}^{surf} = 68.75$ at.%, the surface is purely Ag-terminated.

Finally, we analyzed the influence of configuration entropy by performing canonical Monte Carlo simulations for the Ag-Au (111). **Figure 4** shows the four layers of the simulation cell containing 40×40 atoms in the lateral directions at room temperature for the adsorbate-free surface (a) and the oxygen-covered surface (b). Clearly, the same tendencies as obtained in the
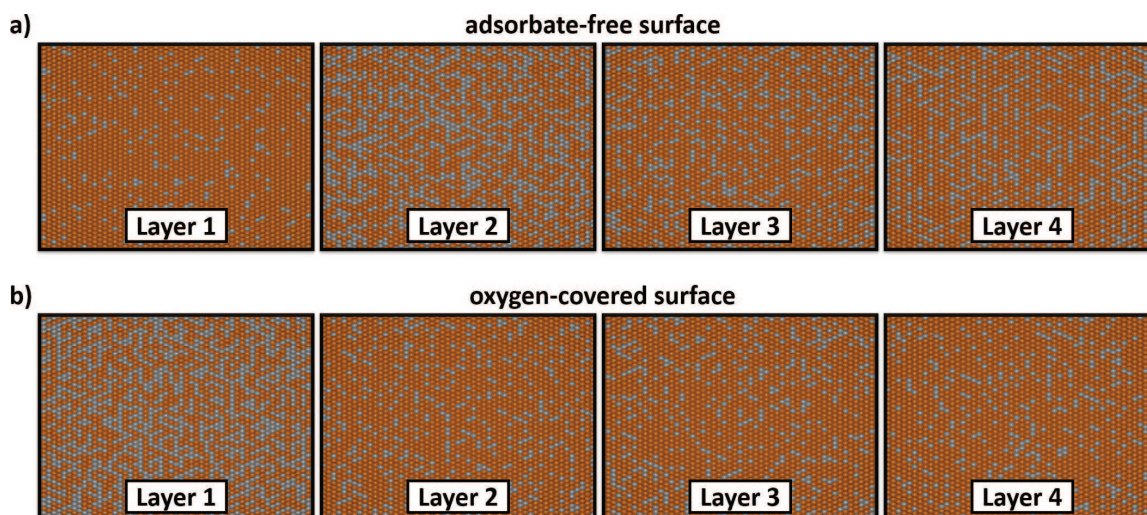
Figure 4. Monte Carlo simulation results at $T = 300$ K for the Ag-Au (111) surface free from adsorbates (a) and with atomic O at an fcc hollow site (b). The first four surface layers of the unit cell containing $40 \times 40 \times 6$ atoms are shown, where layer 1 corresponds to the topmost surface layer.

cluster expansion for $T = 0$ K are still valid at room temperature, even though the long-range order is lost. Without taking into consideration the contribution of phonons, Au enrichment in the topmost layer should be possible to observe in experiments, presuming a thoroughly prepared surface free from adsorbates.

4.2. How silver segregation stabilizes 1D surface gold oxide on the Au (321) surface

Our results for the Ag-Au (111) surface show that the presence of adsorbed oxygen draws Ag to the top surface layer [80]. Ag binds more strongly to O, as it is less noble than Au, and is therefore expected to occupy positions close to the O-adsorbates. Our recently published results [40] on the basis of the CE performed for the stepped Au (321) surface with an infinite oxide chain and Ag impurities resulted in a surprising observation: up to very high Ag surface concentrations of $x_{\text{Ag}}^{\text{surf}} = 87.5$ at.%, the energetically most favorable positions for Ag are located adjacent to the oxide chain, but never within the chain. At Ag surface concentrations lower than that value, atomic positions in the topmost layer next to the chain are first occupied by Ag, followed by positions underneath the chain. When no more direct Ag–O contacts can be created without Ag being located inside the chain, positions at and beneath the edges of the (111) terraces are occupied by Ag. This unexpected behavior can be explained with gold's special electronic structure, namely, the pronounced *s-d* hybridization. The latter leads to a partly covalent bonding character for Au, stabilizing it within the oxide chain. We have characterized the strong, partly covalent Au–O bonds within the chain by analyzing the electronic structure of selected surface configurations.

First, the partial density of states (DOS) reveals strongly overlapping peaks between the Au 5*d* states and the O 2*p* states close to the Au–O bonding and antibonding states in the absence of Ag impurities (see **Figure 5c**). A Ag atom residing next to the infinite oxide chain further increases this overlap, thereby stabilizing Au within the chain (see **Figure 5d**). If Ag occupies

one or both positions inside the chain, the overlap and the covalent bonding character become less pronounced (see **Figure 5a** and **b**). Second, we showed the different nature of the bonding character of an –(O–Au)– chain and an –(O–Ag)– chain by calculating their electron localization functionals (ELF) (see **Figure 6**). The more covalent Au–O bonds manifest themselves in high ELF values around the O atoms as well as the Au atoms and also in the bonding regions. The –(O–Ag)– chain, in contrast, exhibits a small probability for electrons to be located around

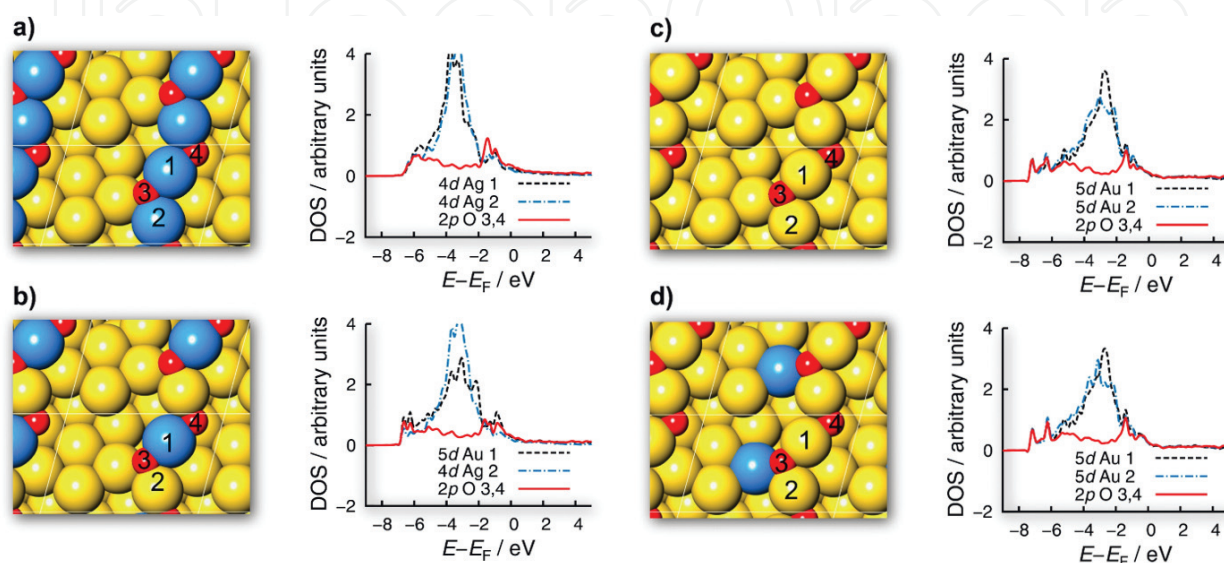**Figure 5.** Partial density of states (DOS) of four surface configurations featuring an –(O–Ag)– chain (a), a mixed oxide chain with alternating Ag and Au atoms (b), an –(O–Au)– chain (c), and an –(O–Au)– chain with Ag atoms adjacent to the chain (d). The corresponding top views of the surface are shown near each diagram. Color code for the top views: Au in yellow, Ag in blue, and O in red. Reproduced from Ref. [40] with permission from the PCCP Owner Societies.
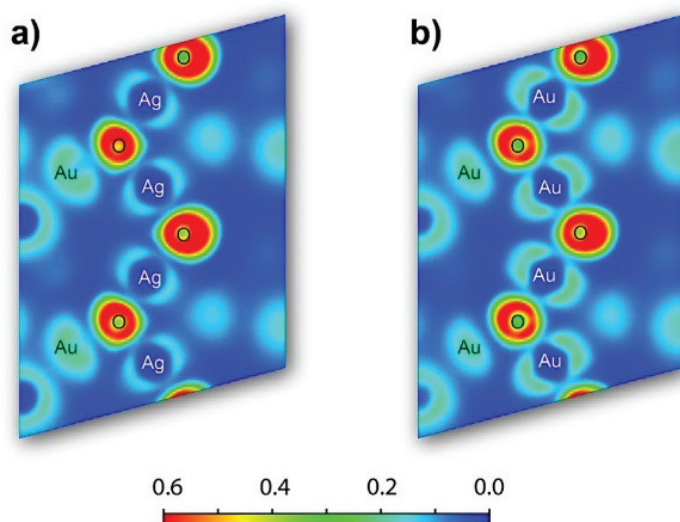

Figure 6. Two-dimensional view of the electron localization function (ELF) for two surface configurations: with an –(O–Ag)– chain (a) and an –(O–Au)– chain (b). Low ELF values are shown in blue, while red areas indicate high ELF values. Reproduced from Ref. [40] with permission from the PCCP Owner Societies.

the Ag atoms and sharp boundaries of the ELF in the bonding regions, indicating a more ionic bonding character. Third, an analysis of the bond lengths within the oxide chain revealed slightly longer bond lengths for Ag–O bonds than for Au–O bonds in the chain, which also suggests a more covalent Au–O bonding character.

Our detailed analysis of the electronic structure of the Au (321) surface with an infinite oxide chain and Ag impurities yields two effects responsible for the obtained ground state configurations: on the one hand, Au is stabilized within the chain by strong, partially covalent Au–O bonds. On the other hand, Ag binds strongly to O and is therefore preferably located close to the O atom. We complemented the cluster expansion study by ab initio molecular dynamics (AIMD) simulations, which support the thermodynamic and electronic structure analyses above.

5. Ab initio MD simulations reveal dynamic surface restructuring

As revealed by our earlier work [94] and incorporated in the analysis above, −(O–Au)– chains are thermodynamically favored over individually adsorbed O atoms on gold. In a recent work [41], we studied the formation of –(O–Au)– chains from adsorbed O atoms by conventional (static) DFT and by DFT-based AIMD simulations. **Figure 7** illustrates an AIMD simulation from a starting structure (0 ps) with several individually adsorbed O atoms placed at their most favorable threefold fcc positions close to step edges of Au (321). After 20 picoseconds of a simulation, a chain consisting of four O atoms linked together was formed. Our simulations were run at an elevated temperature of 700 K to speed up the diffusion and make structural rearrangements as well as the following relaxation happen within the computationally accessible simulation time. AIMD simulations often help us to identify new reaction pathways, such as complex surface rearrangements involving multiple atoms. Approximate transition states and minima identified in a simulation can then be refined by static DFT. The activation barriers for the formation of the first link were calculated to be <0.5 eV, suggesting that this process would take place already at ambient temperature. We have also shown that Ag impurities at low concentration reduce the activation barrier for the –(Au–O)– chain formation, whereas formation of –O–Ag–O– links is energetically slightly unfavorable, especially at high Ag concentration. Interestingly, no chain formation was found on the flat Au (111) surface covered by O atoms at a similar coverage. Hence, the presence of surface steps seems to be crucial for facile –(Au–O)– chain formation.

Once the chains are formed on the surface, they can induce further global restructuring processes, driven by the affinity of Ag atoms to oxygen. The thermodynamic analysis of Refs. [40, 80] summarized in the preceding section revealed two driving forces acting in bimetallic surfaces with adsorbed oxygen. On the one hand, −(Au–O)– chains are thermodynamically preferred over individually adsorbed O on Au, and on the other hand, Ag has a higher affinity to O than Au and Ag–O bonds are more favorable than Au–O bonds.

To study the surface restructuring, which occurs because of these thermodynamic driving forces acting in our bimetallic system with O adsorbate, we carried out AIMD simulations.
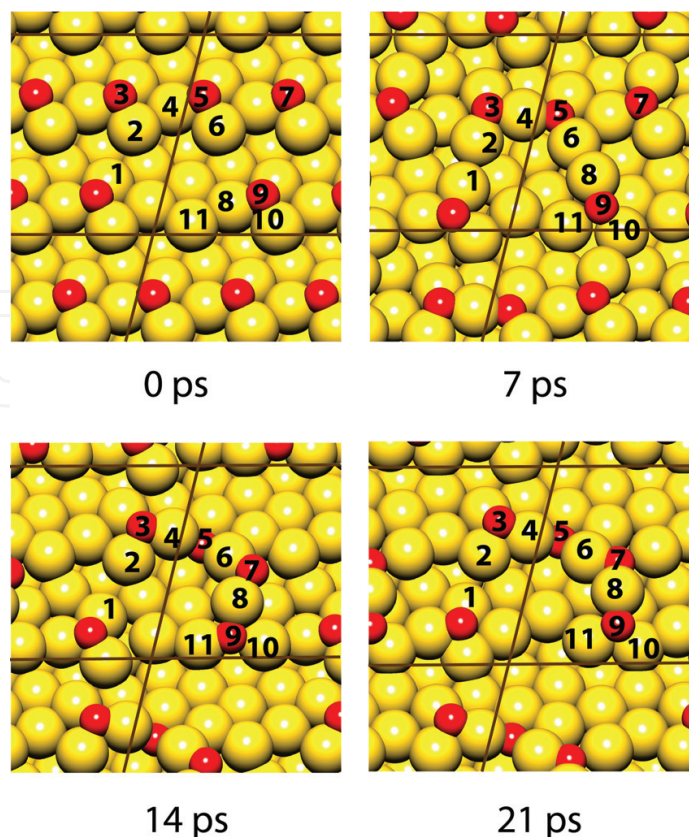
Figure 7. Snapshots of an AIMD simulation showing –(Au–O)– chain formation from individually adsorbed O atoms on Au (321) without Ag impurities. (3 × 2) Unit cell and O coverage of 0.17 ML. Color coding: Au, yellow; O, red. Reproduced with permission from Ref. [39]. Copyright 2017 American Chemical Society.

Two key observations were made in these simulations: first, Ag atoms diffuse towards oxygen of an –(O–Au)– chain and stay in an adjacent position, which shows that the Au–O bonds within the chain are stronger than external Au–O bonds. Second, also the –(O–Au)– chains are able to move towards Ag atoms to maximize the number of external Ag–O contacts, without breaking the internal chain structure [40, 41].

In the simulation illustrated in **Figure 8** [41], we were able to monitor Ag diffusion from subsurface layers to the surface driven by the attractive interaction with two short O–Au–O chains. From **Figure 8**, it can be seen that already after 8 ps a silver atom labeled Ag(**1**) initially located in the subsurface layer directly under the step migrates to the surface and links the two short chains into a longer one. Subsequently, a deeper lying Ag(**2**), initially more than 4 Å away from the surface finds its way to the surface and occupies a position next to one of the O–Au–O fragments. In a reference simulation with a starting structure containing no adsorbed O, no Ag or Au diffusion occurred on the time scale of the simulation. This example illustrated that Ag segregation onto the surface is induced by adsorbed O. Experiments under UHV conditions employing Ag covered stepped Au (332) surface provided evidence in support of our theoretical prediction, showing that oxygen is able to induce surface segregation of Ag already at 200 K [41].
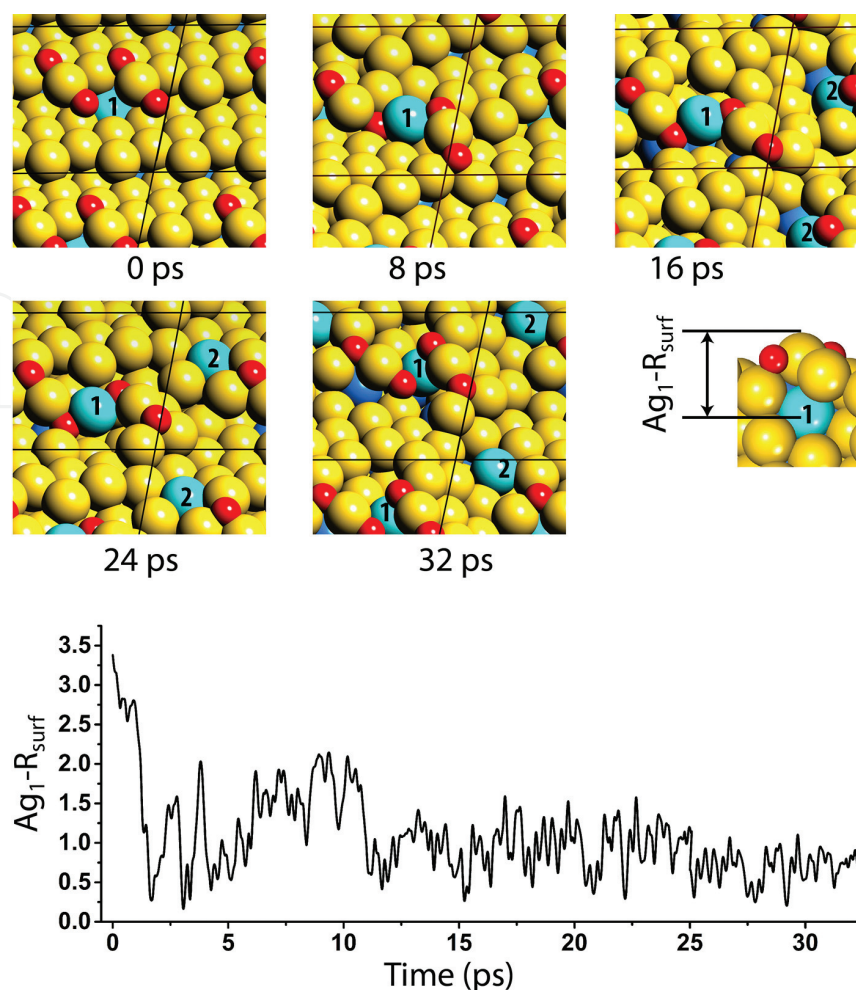
Figure 8. An AIMD simulation showing vertical Ag diffusion from a subsurface layer to the surface. $Ag_1\text{-}R_{surf}$ represents the distance of Ag(1) atom initially located near the step edge to a reference surface. The reference surface is chosen as a Z coordinate slightly above the Au atom of the O–Au–O fragment at 0 ps and is kept fixed during the simulation. Reproduced with permission from Ref. [39]. Copyright 2017 American Chemical Society.

6. Role of surface silver for the catalytic activity of nanoporous gold

Nanostructured gold-based catalysts show unique behavior, being active at sub-ambient temperature and exceptionally selective for partial oxidation and partial hydrogenation reactions [104–106]. These characteristics are also held by npAu, which has been demonstrated to catalyze preferential CO oxidation (PROX) in hydrogen stream [107], oxidative coupling of alcohols to esters [10, 28], cross-coupling reactions of alcohols [108, 109], alcohols and alde-hydes [110, 111], and alcohols and amines [112] at mild conditions. Selective hydrogenation has been little explored on npAu because of generally poor ability of gold to catalyze H_2 dissociation. However, Yamamoto et al. [113] found a way to generate atomic H on npAu by oxidizing organosilanes with water. Using this method of *in situ* hydrogen generation and amine additives, they reached high selectivity and high yields in the selective hydrogenation of

alkynes to alkenes [114] and quinones to 1,2,3,4-hydroquinones [115]. Yamamoto group also reported several C–C coupling reactions catalyzed by npAu [114]. Nevertheless, oxidation reactions remain the main area where npAu is currently being studied as a catalyst. The ability of nanostructured gold to catalyze aerobic oxidation with O_2 as oxidant makes it attractive from the standpoint of "green" chemistry.
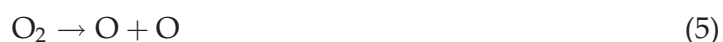
However, the question of how npAu catalyzes O_2 activation and, in particular, whether silver residuals are crucial for the catalytic activity, has been much debated in the literature. Until now, direct experimental evidence justifying a particular mechanism is lacking, although theoretical studies provided valuable insights into possible mechanistic scenarios. In most studies, a dissociative mechanism of O_2 activation has been postulated on npAu, in which O_2 molecule adsorbs dissociatively forming atomic O, which oxidizes adsorbed molecules on the surface in further reaction steps. However, it was difficult to explain, why O_2 can dissociate on npAu, while it does not adsorb or dissociate on extended gold surfaces. Bäumer and co-workers [21] suggested that silver impurities in npAu should assist in the activation of molecular oxygen. Theoretical studies by Moskaleva et al. [39] and Fajín et al. [116] have shown that (i) steps and kinks are crucial for O_2 adsorption and dissociation and (ii) O_2 adsorbs stronger at Ag-rich sites and the activation barrier for O_2 dissociation is reduced at such sites. However, significant lowering of the activation barrier was computationally predicted only for rather large ensembles of >4 Ag atoms, which raised a question of how high is the probability to find such large ensembles, taking into account that the total concentration of residual silver is typically <1 at.% in the bulk. Very recent studies using high-resolution scanning transmission electron microscopy (STEM) combined with elemental mapping using energy-dispersive X-ray spectroscopy (EDXS) shed new light on this question [117, 118]. These two groups independently discovered that Ag is not evenly distributed in npAu but can be concentrated in Ag-rich regions that are probably the fragments of the original Ag-rich master alloy, which evaded corrosion [117]. X-ray photoelectron spectroscopy revealed at least three types of Ag in np-Au samples with different oxidation states or chemical environment, whereas the measured surface content of each type before and after catalytic cycling depended on the sample preparation [119]. Furthermore, theoretical DFT-based studies [41] and experimental studies using Auger and X-ray photoelectron spectroscopies [41, 120] showed that adsorbed surface O should trigger Ag diffusion and enrichment in the surface region. These results indicated that not only Ag impurities, but also atomic O (which is generated in the course of O_2 activation or even already contained in as-prepared samples), may affect the reaction mechanisms on npAu. Recent theoretical studies [41, 94, 121] showed that adsorbed O on gold may be present not only as individual O atoms but also as 1D or 2D chains containing alternating Au and O atoms. Furthermore, theoretical studies demonstrated that the barrier for O_2 dissociation may be lowered significantly as a result of O co-adsorption [94] or due to the formation of Ag-rich regions near –(Au-O)– chains [121]. Therefore, the adsorption energy of O_2 and the activation energy of its dissociation are expected to be very sensitive to the surface composition in terms of Ag and O content as well as the type of phases they form.

Theoretical work [122–124] also suggested a possibility of another mechanism, an associative one, in which O_2 does not dissociate first but reacts directly with CO, water, or methanol, with significantly lower activation energy than required for O_2 dissociation on pure gold and even

on Ag-substituted surfaces. The adsorption of O_2 on extended gold surfaces could be stabilized not only by Ag impurities but also by another admetal, such as Cu [25, 123], as well as through favorable co-adsorption with water or methanol [122, 125]. An especially interesting case is the reaction of O_2 with water, in which water acts as a co-catalyst and helps to dissociate O_2 according to the following reaction sequence:

$$O_2 + H_2O \rightarrow OOH + OH \tag{2}$$

$$OOH \rightarrow O + OH \tag{3}$$

$$2OH \rightarrow O + H_2O \tag{4}$$

The combination of reactions (2)–(4) gives (5):

$$O_2 \rightarrow O + O \tag{5}$$

Hence, water is not consumed in the overall reaction. Because traces of water are often present in the reaction feed, water may be one of the important ingredients, making npAu an active catalyst. In agreement with theoretical predictions, a favorable effect of water co-feed on the activity of CO oxidation on Au nanoparticles and on npAu was observed in catalytic experiments [38, 126].

Several experimental and theoretical studies to date revealed the essential role of Ag impurities for CO oxidation on npAu [21, 37, 39, 116, 121, 127, 128]. For CO oxidation, changing Ag concentration from 1 to 10 at.% increased the activity by more than a factor of 2 at 40°C. However, the presence of Ag may not always be beneficial for the selectivity or perhaps only up to certain Ag concentrations. For instance, increasing Ag content in npAu was shown to reduce the selectivity of gas-phase methanol oxidation towards partial oxidation product methyl formate [10]. Whereas increasing Ag content from <1 to 2.5 at.% worsens the selectivity as the temperature increases [97% (20°C) → 67% (80°C)], further increase of Ag content makes the reaction completely unselective (only CO_2 and H_2O are formed). The drop of the selectivity on npAu with relatively high residual Ag content was attributed to a stronger binding of intermediates on Ag-rich sites, which leads to their fast reaction to total oxidation products (CO, CO_2, and H_2O), whereas low adsorption energy on Au sites allows for a fast desorption of partial oxidation products [10]. Also, for the liquid-phase methanol oxidation at 60°C, the formation of the coupling product was found to be reduced by half when the average Ag content in the whole sample was increased from around 1 to 15 at.%, confirming the above trend. Therefore, optimal concentration of Ag in npAu has to be identified for a particular application to achieve a trade-off between activity and selectivity.

Beyond applications in gas-phase and liquid-phase catalysis, npAu shows good prerequisites (high surface area, high electrical conductivity, good permeability for gas or liquid molecules, ability to host other compounds) for usage in electrocatalysis. In a recent study [119], npAu was investigated in electrocatalysis of methanol. A clear correlation between the content of residual silver and the product distribution, e.g. on the selectivity, was also found in these studies. Samples with higher Ag content favored deeper oxidation product, formate, rather

than formaldehyde. However, the authors also explain that this correlation with Ag content is rather indirect, because samples with high Ag content also had finer ligament and pore size, which, in their opinion, was the decisive property favoring deeper oxidation. Decreasing pore size increased transport limitations, which more strongly affected the two-electron oxidation to HCHO than the four-electron oxidation to HCOO⁻. This example illustrates that not only the surface composition but also the ligament size affects the observed catalytic behavior. Because these two factors are likely related [129], determining the role of Ag independent from other sample properties from experimental studies alone appears to be a tricky task.

7. Outlook on electromechanical coupling at Ag-Au surfaces

In heterogeneous catalysis, the reaction rate typically depends on the dissociative adsorption enthalpy H_{ads} of the key reactant and exhibits a pronounced maximum at a certain H_{ads} value (volcano curve [130, 131]). In 2005, Kibler et al. [132] conducted electrochemical experiments and thereby established a relation between H_{ads} and the electrode lattice spacing. For this purpose, they deposited pseudo-morphic palladium monolayers on seven single-crystal sub-strates with different lattice constants. As the Pd adapted the substrate lattice constant, strain was induced in the monolayers. From voltammetric peak electrode potentials arising from hydrogen desorption, they directly derived the adsorption enthalpy H. Furthermore, they found a linear relation between these peak potentials and a shift of the d-band center, which can be related to strain according to a model by Hammer and Nørskov [133, 134]. In 2011, Weissmüller et al. [135] derived a linear dependence between the peak electrode potential and strain from the data of Kibler et al. and defined a strain response parameter ς_E from the slope:

$$\varsigma_E = \left.\frac{\partial E}{\partial e}\right|_q, \tag{6}$$

where e is the strain and q is the charge density. This response parameter is characteristic for the electrode material and independent of a potential adsorbate used to determine it. The phenomenon described here had already been investigated by Gokhshtein [136, 137], but he did not identify a value for the strain response parameter ς_E at that point.

Due to strain relaxation and the lack of reliable and precise strain measurements, it is usually easier to measure the response ς_f of the surface stress f to the charge density q at the electrode surface [135]. The two response parameters are identical for a surface at equilibrium, as they are connected via a Maxwell relation [138, 139]:

$$\left.\frac{\partial f}{\partial q}\right|_e = \left.\frac{\partial E}{\partial e}\right|_q. \tag{7}$$

Several electrochemical experiments from the past aimed at determining response parameters ς_f for different electrode materials under varying conditions [135, 140–142]. Haiss et al. [140]

conducted voltammetry and surface stress measurements of anions adsorption on the Au (111) surface and obtained a linear correlation between surface stress and interfacial charge at the metal/electrolyte interface. However, the choice of electrolyte influenced the response parameter ς_f and therefore they did not provide a measured value of ς_f. By cantilever bending through electrochemical charging of a (111)-textured gold electrode in solutions of fluoride and perchlorate anions, Smetanin et al. [142] measured a surface stress-charge response parameter of −2 V, which agrees very well with the theoretical value of −1.98 V determined by earlier ab initio calculations [138]. In 2009, Smetanin et al. [143] also determined the strain response parameter ς_E directly via cyclic deformation of a thin gold film on a polymer substrate and by measuring the potential variation. They obtained a value of −1.83 V, which is close to the surface stress-charge response parameter ς_f of −2 V determined in their earlier work [142]. This represents an experimental confirmation of the Maxwell relation in Eq. (7).

Instead of measuring the response of the electrode potential, it is also possible to determine that of the electronic work functional ϕ [138]. The latter describes the work needed to remove an electron from a solid to a point right outside its surface, which is the difference between the vacuum potential and the Fermi level. It has been found that the potential of zero charge of an electrode surface in an electrolyte is closely related to the work functional of a neutral surface in vacuum [144, 145]. The response parameter ς can therefore be calculated from the work functional strain response of a neutral surface without considering an electrolyte in the model system [138]:

$$\varsigma = q_0^{-1} \frac{\partial \phi}{\partial e}\bigg|_{q=0},$$

(8)

where q_0 is the elementary charge $1.6022 \cdot 10^{-19}$ C. In this way, ς can be easily obtained from DFT calculations, as the determination of the work functional is relatively straightforward.

Recently, Albina et al. [146] calculated response parameters for various transition and also noble metals by means of DFT. For the Ag (111) and (100) surfaces, they report values of −2.31 and −0.81 V, respectively. Comparing their results to values for the Au (111) and (100) surfaces (−1.86 and −0.90 V, respectively [138]), the response of the close-packed (111) surface is more pronounced for Ag, while the coefficient for the loosely packed (100) surface has a slightly smaller magnitude for Ag.

While for pure metals, especially gold, the electromechanical coupling phenomenon has been thoroughly studied experimentally as well as in theory, the effect of alloying and more specifically surface segregation remains an open question. The strongly curved npAu surface probably contains numerous strained areas, where the catalytic reactivity may be different from the unstrained surface. Furthermore, systematically straining the material to tune the reactivity may be an attractive option. Therefore, it is crucial to understand the influence of the presence of a second metal on the electromechanical coupling behavior.

We have performed cluster expansions for different Ag-Au surfaces as well as for a varying Ag bulk concentration to determine energetically favorable configurations. Since the electromechanical

coupling coefficient is a quantity that depends on the surface configuration, it can also be expanded by means of the cluster expansion. We can then combine the two expansions and find out how surface formation enthalpy and electromechanical coupling are related. For this purpose, we will apply small strain values to our surface slabs and additionally account for contraction in the direction of the surface normal. The corresponding equilibrium interlayer spacings for the bulk layers emerge from Murnaghan fits [147] for strained bulk cells. The work functional ϕ is subsequently determined for different strain values by calculating the difference between the vacuum potential outside the surface V_{vac} and the Fermi level E_{F}. Our goal is to analyze the influence of a varying Ag bulk concentration, Ag surface concentration, and the surface configuration on the electromechanical coupling parameter. We expect the values of ς to lie between those of pure Ag and Au, i.e. between -2.31 and -1.86 V for the (111) surface. We are currently in the process of finalizing this study, which will be fully covered in a forthcoming publication [148].

8. Conclusions

Nanoporous gold (npAu) is a fascinating material with intriguing properties and an immense potential for controlled modification and design of smart materials. At first glance, this porous noble metal seems to be astonishingly simple, but a closer look at it reveals a rather complex surface composition and rich surface chemistry. The knowledge gained over the past decades regarding the structure, composition, and reactivity of npAu brought us further in our understanding of this material but at the same time posed new questions to be answered in future studies.

Twelve years after the discovery of its catalytic activity, npAu is now widely regarded as a bimetallic catalyst, since the role of a residual less noble metal for its activity has been recognized as essential. In this chapter, we discussed silver as the second (minor) metal component and commented on its role for oxidation catalysis. However, the focus of this review has been on the theoretical and experimental studies of Ag segregation in npAu and in Ag-Au model surfaces. Particularly, we were interested in segregation induced by the presence of O adsorbates. Therefore, a detailed overview of experimental and theoretical studies on surface segregation in Ag-Au systems has been presented here. While most previous investigations report either no segregation or a slight Ag enrichment in the surface, our own theoretical analysis predicted thermodynamically favorable Au termination for Au-Ag (111) surfaces in the absence of surface O. We also demonstrated that chemisorbed atomic oxygen draws Ag to the surface. The diffusion and restructuring processes were predicted to be facilitated by a stepped surface structure. For such stepped surfaces, Ag diffusion is fast enough to happen on the time scale of catalytic experiments, as demonstrated by Auger spectroscopy already at 200 K. Because in oxidation catalysis, the surface of a catalyst is expected to be covered by oxygen atoms, oxygen-driven Ag segregation would result in a silver enriched surface.

Our theoretical work discussed here revealed that O atoms at Au-rich Au-Ag surfaces may dynamically form –(O–Au)– chain structures, which are thermodynamically preferred over individually adsorbed O and that Ag atoms tend to occupy positions next to –(O–Au)– chains.

Such small assemblages of Ag impurities near the oxide chains may serve as reactive sites, e.g. for the dissociation of O_2.

Experimental evidence from catalytic studies on np-Au shows that these catalysts are exceptionally selective towards partial oxidation, which is a unique property of Au catalysts; however, increasing Ag concentration favors deep oxidation and hence deteriorates the selectivity towards partial oxidation products. At the same time, increasing Ag content was found beneficial for enhancing the overall activity and was suggested to improve the stability against catalysis-induced ligament coarsening.

Finally, we presented an outlook on electromechanical coupling at Ag-Au surfaces, which may provide a possibility to systematically tune the catalytic activity of bimetallic surfaces. We are currently investigating the effect of Ag admetal on the electromechanical coupling parameter.

Acknowledgements

Author details

Sandra Hoppe[1] and Lyudmila V. Moskaleva[2]*

*Address all correspondence to: moskaleva@uni-bremen.de

1 Institute of Advanced Ceramics, Hamburg University of Technology, Hamburg, Germany

2 Institute of Applied Physical Chemistry and Center for Environmental Research, University of Bremen, Bremen, Germany

References

[1] Bond GC, Louis C, Thompson DT. Catalysis by Gold. London, Singapore: Imperial College Press; 2006

[2] Cha DY, Parravano G. Surface reactivity of supported gold: I. Oxygen transfer between CO and CO_2. Journal of Catalysis. 1970;**18**(2):200-211. DOI: 10.1016/0021-9517(70)90178-8

[3] Bond GC, Sermon PA. Gold catalysts for olefin hydrogenation. Gold Bulletin. 1973;**6**(4): 102-105. DOI: 10.1007/BF03215018

[4]   Bond GC, Sermon PA, Webb G, Buchanan DA, Wells PB. Hydrogenation over supported gold catalysts. Journal of the Chemical Society, Chemical Communications. 1973;(13): 444-445. DOI: 10.1039/C3973000444B

[5]   Galvagno S, Parravano G. Chemical reactivity of supported gold: IV. Reduction of NO by H_2. Journal of Catalysis. 1978;**55**(2):178-190. DOI: 10.1016/0021-9517(78)90204-X

[6]   Hutchings GJ. Vapor phase hydrochlorination of acetylene: Correlation of catalytic activity of supported metal chloride catalysts. Journal of Catalysis. 1985;**96**(1):292-295. DOI: 10.1016/0021-9517(85)90383-5

[7]   Haruta M, Kobayashi T, Sano H, Yamada N. Novel gold catalysts for the oxidation of carbon monoxide at a temperature far below 0°C. Chemistry Letters. 1987;**16**(2):405-408. DOI: 10.1246/cl.1987.405

[8]   Haruta M. When gold is not noble: Catalysis by nanoparticles. Chemical Record. 2003; **3**(2):75-87. DOI: 10.1002/tcr.10053

[9]   Freyschlag CG, Madix RJ. Precious metal magic: Catalytic wizardry. Materials Today. 2011;**14**(4):134-142. DOI: 10.1016/S1369-7021(11)70085-2

[10] Wittstock A, Zielasek V, Biener J, Friend CM, Bäumer M. Nanoporous gold catalysts for selective gas-phase oxidative coupling of methanol at low temperature. Science. 2010; **327**(5963):319-322. DOI: 10.1126/science.1183591

[11] Liu J-H, Wang A-Q, Chi Y-S, Lin H-P, Mou C-Y. Synergistic effect in an Au-Ag alloy nanocatalyst: CO oxidation. The Journal of Physical Chemistry. B. 2005;**109**(1):40-43. DOI: 10.1021/jp044938g

[12] Wang A-Q, Liu J-H, Lin SD, Lin T-S, Mou C-Y. A novel efficient Au-Ag alloy catalyst system: Preparation, activity, and characterization. Journal of Catalysis. 2005;**233**(1):186-197. DOI: 10.1016/j.jcat.2005.04.028

[13] Liu X, Wang A, Yang X, et al. Synthesis of thermally stable and highly active bimetallic Au-Ag nanoparticles on inert supports. Chemistry of Materials. 2009;**21**(2):410-418. DOI: 10.1021/cm8027725

[14] Yen C-W, Lin M-L, Wang A, Chen S-A, Chen J-M, Mou C-Y. CO oxidation catalyzed by Au-Ag bimetallic nanoparticles supported in *Mesoporous silica*. Journal of Physical Chemistry C. 2009;**113**(41):17831-17839. DOI: 10.1021/jp9037683

[15] Sandoval A, Aguilar A, Louis C, Traverse A, Zanella R. Bimetallic Au-Ag/TiO_2 catalyst prepared by deposition-precipitation: High activity and stability in CO oxidation. Journal of Catalysis. 2011;**281**(1):40-49. DOI: 10.1016/j.jcat.2011.04.003

[16] Iizuka Y, Kawamoto A, Akita K, et al. Effect of impurity and pretreatment conditions on the catalytic activity of Au powder for CO oxidation. Catalysis Letters. 2004;**97**(3/4):203-208. DOI: 10.1023/B:CATL.0000038585.12878.9a

[17] Hutchings GJ. Catalysis by gold. Catalysis Today. 2005;**100**(1–2):55-61. DOI: 10.1016/j. cattod.2004.12.016

[18] Ding Y, Kim Y-J, Erlebacher J. Nanoporous gold leaf: "Ancient technology"/advanced material. Advanced Materials. 2004;**16**(21):1897-1900. DOI: 10.1002/adma.200400792

[19] Seker E, Reed ML, Begley MR. Nanoporous gold: Fabrication, characterization, and applications. Materials. 2009;**2**(4):2188-2215. DOI: 10.3390/ma2042188

[20] Scaglione F, Rizzi P, Celegato F, Battezzati L. Synthesis of nanoporous gold by free corrosion of an amorphous precursor. Journal of Alloys and Compounds. 2014;**615**: S142-S147. DOI: 10.1016/j.jallcom.2014.01.239

[21] Zielasek V, Jürgens B, Schulz C, et al. Gold catalysts: Nanoporous gold foams. Angewandte Chemie, International Edition. 2006;**45**(48):8241-8244. DOI: 10.1002/anie.200602484

[22] Jürgens B, Kübel C, Schulz C, et al. New gold and silver-gold catalysts in the shape of sponges and sieves. Gold Bulletin. 2007;**40**(2):142-149. DOI: 10.1007/BF03215571

[23] Xu C, Su J, Xu X, et al. Low temperature CO oxidation over unsupported nanoporous gold. Journal of the American Chemical Society. 2007;**129**(1):42-43. DOI: 10.1021/ja0675503

[24] Wittstock A, Wichmann A, Bäumer M. Nanoporous gold as a platform for a building block catalyst. ACS Catalysis. 2012;**2**(10):2199-2215. DOI: 10.1021/cs300231u

[25] Wang L-C, Zhong Y, Jin H, Widmann D, Weissmüller J, Behm RJ. Catalytic activity of nanostructured Au: Scale effects versus bimetallic/bifunctional effects in low-temperature CO oxidation on nanoporous Au. Beilstein Journal of Nanotechnology. 2013;**4**:111-128. DOI: 10.3762/bjnano.4.13

[26] Wittstock A, Bäumer M. Catalysis by unsupported skeletal gold catalysts. Accounts of Chemical Research. 2014;**47**(3):731-739. DOI: 10.1021/ar400202p

[27] Bipp H, Kieczka H. Formamides. In: Ullmann's Encyclopedia of Industrial Chemistry, Electronic Release. Weinheim: Wiley-VCH; 2000

[28] Personick ML, Zugic B, Biener MM, Biener J, Madix RJ, Friend CM. Ozone-activated nanoporous gold: A stable and storable material for catalytic oxidation. ACS Catalysis. 2015;**5**(7):4237-4241. DOI: 10.1021/acscatal.5b00330

[29] Yamamoto Y. Perspectives on organic synthesis using nanoporous metal skeleton catalysts. Tetrahedron. 2014;**70**(14):2305-2317. DOI: 10.1016/j.tet.2013.09.065

[30] Kim SH. Nanoporous gold films as catalyst. In: Mishra NK, editor. Catalytic Application of Nano-Gold Catalysts. Rijeka: InTech; 2016. Ch. 01

[31] Fujita T, Guan P, McKenna K, et al. Atomic origins of the high catalytic activity of nanoporous gold. Nature Materials. 2012;**11**(9):775-780. DOI: 10.1038/nmat3391

[32] Pireaux JJ, Chtaïb M, Delrue JP, Thiry PA, Liehr M, Caudano R. Electron spectroscopic characterization of oxygen adsorption on gold surfaces. Surface Science. 1984;**141**(1):211-220. DOI: 10.1016/0039-6028(84)90206-1

[33] Saliba N, Parker D, Koel B. Adsorption of oxygen on Au(111) by exposure to ozone. Surface Science. 1998;**410**(2):270-282. DOI: 10.1016/S0039-6028(98)00309-4

[34] Kim J, Samano E, Koel BE. Oxygen adsorption and oxidation reactions on Au(211) surfaces: Exposures using O_2 at high pressures and ozone (O_3) in UHV. Surface Science. 2006;**600**(19):4622-4632. DOI: 10.1016/j.susc.2006.07.057

[35] Gong J, Flaherty DW, Ojifinni RA, White JM, Mullins CB. Surface chemistry of methanol on clean and atomic oxygen pre-covered Au(111). Journal of Physical Chemistry C. 2008; **112**(14):5501-5509. DOI: 10.1021/jp0763735

[36] Haruta M. New generation of gold catalysts: Nanoporous foams and tubes – Is unsupported gold catalytically active? ChemPhysChem. 2007;**8**(13):1911-1913. DOI: 10.1002/cphc.200700325

[37] Wittstock A, Neumann B, Schaefer A, et al. Nanoporous Au: An unsupported pure gold catalyst? Journal of Physical Chemistry C. 2009;**113**(14):5593-5600. DOI: 10.1021/jp808185v

[38] Wittstock A, Biener J, Baumer M. Nanoporous gold: A new material for catalytic and sensor applications. Physical Chemistry Chemical Physics. 2010;**12**(40):12919-12930. DOI: 10.1039/C0CP00757A

[39] Moskaleva LV, Röhe S, Wittstock A, et al. Silver residues as a possible key to a remarkable oxidative catalytic activity of nanoporous gold. Physical Chemistry Chemical Physics. 2011;**13**(10):4529-4539. DOI: 10.1039/c0cp02372h

[40] Hoppe S, Li Y, Moskaleva LV, Müller S. How silver segregation stabilizes 1D surface gold oxide: A cluster expansion study combined with ab initio MD simulations. Physical Chemistry Chemical Physics. 2017;**19**(22):14845-14853. DOI: 10.1039/c7cp02221b

[41] Li Y, Dononelli W, Moreira R, et al. Oxygen-driven surface evolution of nanoporous gold: Insights from Ab initio molecular dynamics and Auger electron spectroscopy. Journal of Physical Chemistry C. 2017. DOI: 10.1021/acs.jpcc.7b08873

[42] Dowben PA, Miller A, editors. Surface Segregation Phenomena. Boca Raton, FL.: CRC Press; 1990

[43] Polak M. Surface segregation. Journal of Physics: Condensed Matter. 2016;**28**(6):60301

[44] van Santen RA, Sachtler W. A theory of surface enrichment in ordered alloys. Journal of Catalysis. 1974;**33**(2):202-209. DOI: 10.1016/0021-9517(74)90264-4

[45] Burton JJ, Hyman E, Fedak DG. Surface segregation in alloys. Journal of Catalysis. 1975; **37**(1):106-113. DOI: 10.1016/0021-9517(75)90138-4

[46] Overbury SH, Bertrand PA, Somorjai GA. Surface composition of binary systems. Prediction of surface phase diagrams of solid solutions. Chemical Reviews. 1975;**75**(5):547-560. DOI: 10.1021/cr60297a001

[47] Williams FL, Nason D. Binary alloy surface compositions from bulk alloy thermodynamic data. Surface Science. 1974;**45**(2):377-408. DOI: 10.1016/0039-6028(74)90177-0

[48] Balseiro CA, Morán-López JL. Electronic theory for surface segregation: Noble-metal alloys. Physical Review B. 1980;**21**(2):349-354. DOI: 10.1103/PhysRevB.21.349

[49] Wynblatt P, Ku RC. Surface energy and solute strain energy effects in surface segregation. Surface Science. 1977;**65**(2):511-531. DOI: 10.1016/0039-6028(77)90462-9

[50] Abraham FF, Nan-Hsiung T, Pound GM. Bond and strain energy effects in surface segregation: An atomic calculation. Surface Science. 1979;**83**(2):406-422. DOI: 10.1016/0039-6028(79)90053-0

[51] Dowben PA, Miller AH, Vook RW. Surface segregation from gold alloys. Gold Bulletin. 1987;**20**(3):54-65. DOI: 10.1007/BF03214658

[52] Suh I-K, Ohta H, Waseda Y. High-temperature thermal expansion of six metallic elements measured by dilatation method and X-ray diffraction. Journal of Materials Science. 1988;**23**(2):757-760. DOI: 10.1007/BF01174717

[53] Kittel C. Introduction to Solid State Physics. 8th ed. Hoboken, NJ: Wiley; 2005

[54] Overbury S, Somorjai G. The surface composition of the silver-gold system by Auger electron spectroscopy. Surface Science. 1976;**55**(1):209-226. DOI: 10.1016/0039-6028(76)90385-X

[55] Yabumoto M, Watanabe K, Yamashina T. An AES study of surface segregation of Ag-Au alloys with ion bombardment and annealing. Surface Science. 1978;**77**(3):615-625. DOI: 10.1016/0039-6028(78)90145-0

[56] Bouwman R, Toneman L, Boersma M, van Santen R. Surface enrichment in Ag-Au alloys. Surface Science. 1976;**59**(1):72-82. DOI: 10.1016/0039-6028(76)90292-2

[57] Fain SC, McDavid JM. Work-function variation with alloy composition: Ag-Au. Physical Review B. 1974;**9**(12):5099-5107. DOI: 10.1103/PhysRevB.9.5099

[58] Somorjai GA, Overbury SH. Auger electron spectroscopy of alloy surfaces. Faraday Discussions of the Chemical Society. 1975;**60**:279. DOI: 10.1039/dc9756000279

[59] Nelson G. Determination of the surface versus bulk composition of silver-gold alloys by low energy ion scattering spectroscopy. Surface Science. 1976;**59**(1):310-314. DOI: 10.1016/0039-6028(76)90310-1

[60] Kelley MJ, Swartzfager DG, Sundaram VS. Surface segregation in the Ag-Au and Pt-Cu systems. Journal of Vacuum Science and Technology. 1979;**16**(2):664-667. DOI: 10.1116/1.570052

[61] King TS, Donnelly RG. Surface compositions and composition profiles of Ag-Au (100), (110), and (111) surfaces determined quantitatively by Auger electron spectroscopy. Surface Science. 1985;**151**(2):374-399. DOI: 10.1016/0039-6028(85)90382-6

[62] Meinel K, Klaua M, Bethge H. Segregation and sputter effects on perfectly smooth (111) and (100) surfaces of Au-Ag alloys studied by AES. Physica Status Solidi A. 1988;**106**(1):133-144. DOI: 10.1002/pssa.2211060117

[63] Derry GN, Wan R. Comparison of surface structure and segregation in AgAu and NiPd alloys. Surface Science. 2004;**566–568**:862-868. DOI: 10.1016/j.susc.2004.06.022

[64] Bozzolo G, Garcés JE, Derry GN. Atomistic modeling of segregation and bulk ordering in Ag-Au alloys. Surface Science. 2007;**601**(9):2038-2046. DOI: 10.1016/j.susc.2007.02.035

[65] Cheng D, Liu X, Cao D, Wang W, Huang S. Surface segregation of Ag-Cu-Au trimetallic clusters. Nanotechnology. 2007;**18**(47):475702. DOI: 10.1088/0957-4484/18/47/475702

[66] Curley BC, Rossi G, Ferrando R, Johnston RL. Theoretical study of structure and segregation in 38-atom Ag-Au nanoalloys. European Physical Journal D: Atomic, Molecular, Optical and Plasma Physics. 2007;**43**(1–3):53-56. DOI: 10.1140/epjd/e2007-00091-y

[67] Deng L, Hu W, Deng H, Xiao S, Tang J. Au-Ag bimetallic nanoparticles: Surface segregation and atomic-scale structure. Journal of Physical Chemistry C. 2011;**115**(23):11355-11363. DOI: 10.1021/jp200642d

[68] Bonačić-Koutecký V, Burda J, Mitrić R, Ge M, Zampella G, Fantucci P. Density functional study of structural and electronic properties of bimetallic silver-gold clusters: Comparison with pure gold and silver clusters. The Journal of Chemical Physics. 2002;**117**(7): 3120-3131. DOI: 10.1063/1.1492800

[69] Mitrić R, Bürgel C, Burda J, Bonačić-Koutecký V, Fantucci P. Structural properties and reactivity of bimetallic silver-gold clusters. European Physical Journal D: Atomic, Molecular, Optical and Plasma Physics. 2003;**24**(1):41-44. DOI: 10.1140/epjd/e2003-00124-7

[70] Weis P, Welz O, Vollmer E, Kappes MM. Structures of mixed gold-silver cluster cations $(Ag(m)Au(n)^+$, m + n < 6): Ion mobility measurements and density-functional calculations. The Journal of Chemical Physics. 2004;**120**(2):677-684. DOI: 10.1063/1.1630568

[71] Zhang M, Fournier R. Structure of 55-atom bimetallic clusters. THEOCHEM. 2006; **762**(1):49-56. DOI: 10.1016/j.theochem.2005.08.042

[72] Chen F, Johnston RL. Charge transfer driven surface segregation of gold atoms in 13-atom Au-Ag nanoalloys and its relevance to their structural, optical and electronic properties. Acta Materialia. 2008;**56**(10):2374-2380. DOI: 10.1016/j.actamat.2008.01.048

[73] Paz-Borbón LO, Johnston RL, Barcaro G, Fortunelli A. Structural motifs, mixing, and segregation effects in 38-atom binary clusters. The Journal of Chemical Physics. 2008; **128**(13):134517. DOI: 10.1063/1.2897435

[74] Dianat A, Zimmermann J, Seriani N, Bobeth M, Pompe W, Ciacchi LC. Ab initio study of element segregation and oxygen adsorption on PtPd and CoCr binary alloy surfaces. Surface Science. 2008;**602**(4):876-884. DOI: 10.1016/j.susc.2007.12.016

[75] Bader RFW. Atoms in Molecules: A Quantum Theory. Reprinted. Oxford [England]: Clarendon Press; 2003. cop. 1990

[76] Henkelman G, Arnaldsson A, Jónsson H. A fast and robust algorithm for Bader decomposition of charge density. Computational Materials Science. 2006;**36**(3):354-360. DOI: 10.1016/j.commatsci.2005.04.010

[77] Sanville E, Kenny SD, Smith R, Henkelman G. Improved grid-based algorithm for Bader charge allocation. Journal of Computational Chemistry. 2007;**28**(5):899-908. DOI: 10.1002/jcc.20575

[78] Tang W, Sanville E, Henkelman G. A grid-based Bader analysis algorithm without lattice bias. Journal of Physics: Condensed Matter. 2009;**21**(8):84204. DOI: 10.1088/0953-8984/21/8/084204

[79] Friedel J. The physics of clean metal surfaces. Annals of Physics. 1976;**1**:257-307. DOI: 10.1051/anphys/197601060257

[80] Hoppe S, Müller S. A first principles study on the electronic origins of silver segregation at the Ag-Au (111) surface. Journal of Applied Physics. 2017;**122**:235303. DOI: 10.1063/1.5017959

[81] Sholl DS, Steckel JA. Density Functional Theory. Hoboken, NJ, USA: John Wiley & Sons, Inc.; 2009

[82] Kresse G, Hafner J. Ab initio molecular dynamics for liquid metals. Physical Review B. 1993;**47**(1):558-561. DOI: 10.1103/PhysRevB.47.558

[83] Kresse G, Hafner J. Norm-conserving and ultrasoft pseudopotentials for first-row and transition elements. Journal of Physics: Condensed Matter. 1994;**6**(40):8245

[84] Kresse G, Furthmüller J. Efficient iterative schemes for ab initio total-energy calculations using a plane-wave basis set. Physical Review B. 1996;**54**(16):11169-11186. DOI: 10.1103/PhysRevB.54.11169

[85] Kresse G, Joubert D. From ultrasoft pseudopotentials to the projector augmented-wave method. Physical Review B. 1999;**59**(3):1758-1775. DOI: 10.1103/PhysRevB.59.1758

[86] VandeVondele J, Krack M, Mohamed F, Parrinello M, Chassaing T, Hutter J. Quickstep: Fast and accurate density functional calculations using a mixed Gaussian and plane waves approach. Computer Physics Communications. 2005;**167**(2):103-128. DOI: 10.1016/j.cpc.2004.12.014

[87] Perdew JP. Density-functional approximation for the correlation energy of the inhomogeneous electron gas. Physical Review B. 1986;**33**(12):8822-8824. DOI: 10.1103/PhysRevB.33.8822

[88] Perdew JP, Burke K, Wang Y. Generalized gradient approximation for the exchange-correlation hole of a many-electron system. Physical Review B. 1996;**54**(23):16533-16539. DOI: 10.1103/PhysRevB.54.16533

[89] Grimme S, Antony J, Ehrlich S, Krieg H. A consistent and accurate ab initio parametrization of density functional dispersion correction (DFT-D) for the 94 elements H-Pu. The Journal of Chemical Physics. 2010;**132**(15):154104. DOI: 10.1063/1.3382344

[90] Shi H, Stampfl C. First-principles investigations of the structure and stability of oxygen adsorption and surface oxide formation at Au(111). Physical Review B. 2007;**76**(7):27. DOI: 10.1103/PhysRevB.76.075327

[91] Baker TA, Xu B, Liu X, Kaxiras E, Friend CM. Nature of oxidation of the Au(111) surface: Experimental and theoretical investigation. Journal of Physical Chemistry C. 2009;**113**(38):16561-16564. DOI: 10.1021/jp9052192

[92] Landmann M, Rauls E, Schmidt WG. Chainlike Au-O structures on Au(110) − (1 × r) surfaces calculated from first principles. Journal of Physical Chemistry C. 2009;**113**(14): 5690-5699. DOI: 10.1021/jp810581s

[93] Hiebel F, Montemore MM, Kaxiras E, Friend CM. Direct visualization of quasi-ordered oxygen chain structures on Au(110) − (1 × 2). Surface Science 2016;**650**:5-10. DOI: 10.1016/j.susc.2015.09.018

[94] Moskaleva LV, Weiss T, Klüner T, Bäumer M. Chemisorbed oxygen on the Au(321) surface alloyed with silver: A first-principles investigation. Journal of Physical Chemistry C. 2015;**119**(17):9215-9226. DOI: 10.1021/jp511884k

[95] Moskaleva LV, Zielasek V, Klüner T, Neyman KM, Bäumer M. CO oxidation by co-adsorbed atomic O on the Au(321) surface with Ag impurities: A mechanistic study from first-principles calculations. Chemical Physics Letters. 2012;**525-526**:87-91. DOI: 10.1016/j. cplett.2011.12.050

[96] Nosé S. A unified formulation of the constant temperature molecular dynamics methods. The Journal of Chemical Physics. 1984;**81**(1):511-519. DOI: 10.1063/1.447334

[97] Hoover WG. Canonical dynamics: Equilibrium phase-space distributions. Physical Review A. 1985;**31**(3):1695-1697

[98] Sanchez JM, Ducastelle F, Gratias D. Generalized cluster description of multicomponent systems. Physica A: Statistical Mechanics and its Applications. 1984;**128**(1–2):334-350. DOI: 10.1016/0378-4371(84)90096-7

[99] Lerch D, Wieckhorst O, Hart GLW, Forcade RW, Müller S. UNCLE: A code for constructing cluster expansions for arbitrary lattices with minimal user-input. Modelling and Simulation in Materials Science and Engineering. 2009;**17**(5):55003

[100] Blum V, Hart GLW, Walorski MJ, Zunger A. Using genetic algorithms to map first-principles results to model Hamiltonians: Application to the generalized Ising model for alloys. Physical Review B. 2005;**72**(16):165113

[101] Hart GLW, Blum V, Walorski MJ, Zunger A. Evolutionary approach for determining first-principles hamiltonians. Nature Materials. 2005;**4**(5):391-394. DOI: 10.1038/nmat1374

[102] Hart GLW, Forcade RW. Generating derivative structures from multilattices: Algorithm and application to hcp alloys. Physical Review B. 2009;**80**(1):14120

[103] Hart GL, Nelson LJ, Forcade RW. Generating derivative structures at a fixed concentration. Computational Materials Scienc. 2012;**59**(Supplement C):101-107. DOI: 10.1016/j. commatsci.2012.02.015

[104] Corma A, Garcia H. Supported gold nanoparticles as catalysts for organic reactions. Chemical Society Reviews. 2008;**37**(9):2096-2126. DOI: 10.1039/B707314N

[105] Sharma AS, Kaur H, Shah D. Selective oxidation of alcohols by supported gold nanoparticles: Recent advances. RSC Advances. 2016;**6**(34):28688-28727. DOI: 10.1039/ C5RA25646A

[106] Mallat T, Baiker A. Potential of gold nanoparticles for oxidation in fine chemical synthesis. Annual Review of Chemical and Biomolecular Engineering. 2012;**3**(1):11-28. DOI: 10.1146/annurev-chembioeng-062011-081046

[107] Li D, Zhu Y, Wang H, Ding Y. Nanoporous gold as an active low temperature catalyst toward CO oxidation in hydrogen-rich stream. Scientific Reports. 2013;**3**:3015 EP. DOI: 10.1038/srep03015

[108] Wang L-C, Stowers KJ, Zugic B, et al. Exploiting basic principles to control the selectivity of the vapor phase catalytic oxidative cross-coupling of primary alcohols over nanoporous gold catalysts. Journal of Catalysis. 2015;**329**(Supplement C):78-86. DOI: 10.1016/j.jcat.2015.04.022

[109] Stowers KJ, Madix RJ, Biener MM, Biener J, Friend CM. Facile ester synthesis on Ag-modified nanoporous Au: Oxidative coupling of ethanol and 1-Butanol under UHV conditions. Catalysis Letters. 2015;**145**(6):1217-1223. DOI: 10.1007/s10562-015-1525-4

[110] Wang L-C, Stowers KJ, Zugic B, et al. Methyl ester synthesis catalyzed by nanoporous gold: From 10-9 Torr to 1 atm. Catalysis Science & Technology. 2015;**5**(2):1299-1306. DOI: 10.1039/C4CY01169D

[111] Lackmann A, Mahr C, Schowalter M, et al. A comparative study of alcohol oxidation over nanoporous gold in gas and liquid phase. Journal of Catalysis. 2017;**353**(Supplement C):99-106. DOI: 10.1016/j.jcat.2017.07.008

[112] Wichmann A, Bäumer M, Wittstock A. Oxidative coupling of alcohols and amines over bimetallic unsupported nanoporous gold: Tailored activity through mechanistic predictability. ChemCatChem. 2015;**7**(1):70-74. DOI: 10.1002/cctc.201402843

[113] Asao N, Ishikawa Y, Hatakeyama N, et al. Nanostructured materials as catalysts: Nanoporous-gold-catalyzed oxidation of organosilanes with water. Angewandte Chemie, International Edition. 2010;**49**(52):10093-10095. DOI: 10.1002/anie.201005138

[114] Yan M, Jin T, Ishikawa Y, et al. Nanoporous gold catalyst for highly selective Semihydrogenation of alkynes: Remarkable effect of amine additives. Journal of the American Chemical Society. 2012;**134**(42):17536-17542. DOI: 10.1021/ja3087592

[115] Yan M, Jin T, Chen Q, et al. Unsupported nanoporous gold catalyst for highly selective hydrogenation of quinolines. Organic Letters. 2013;**15**(7):1484-1487. DOI: 10.1021/ol400229z

[116] Fajín JLC, Cordeiro MNDS, Gomes JRB. On the theoretical understanding of the unexpected O_2 activation by nanoporous gold. Chemical Communications. 2011;**47**(29):8403-8405. DOI: 10.1039/C1CC12166A

[117] Krekeler T, Straßer AV, Graf M, et al. Silver-rich clusters in nanoporous gold. Materials Research Letters. 2017;**5**(5):314-321. DOI: 10.1080/21663831.2016.1276485

[118] Mahr C, Kundu P, Lackmann A, et al. Quantitative determination of residual silver distribution in nanoporous gold and its influence on structure and catalytic performance. Journal of Catalysis. 2017;**352**:52-58. DOI: 10.1016/j.jcat.2017.05.002

[119] Graf M, Haensch M, Carstens J, Wittstock G, Weissmuller J. Electrocatalytic methanol oxidation with nanoporous gold: Microstructure and selectivity. Nanoscale. 2017;**9**(45): 17839-17848. DOI: 10.1039/C7NR05124G

[120] Schaefer A, Ragazzon D, Wittstock A, et al. Toward controlled modification of nanoporous gold. A detailed surface science study on cleaning and oxidation. Journal of Physical Chemistry C. 2012;**116**(7):4564-4571. DOI: 10.1021/jp207638t

[121] Montemore MM, Madix RJ, Kaxiras E. How does nanoporous gold dissociate molecular oxygen? Journal of Physical Chemistry C. 2016;**120**(30):16636-16640. DOI: 10.1021/acs. jpcc.6b03371

[122] Dononelli W, Klüner T, Moskaleva L. Understanding the oxygen activation on nanoporous gold (in preparation)

[123] Dononelli W, Klüner T. CO oxidation over unsupported group 11 metal catalysts: New mechanistic insight from first principles. Faraday Discussions. 2018, accepted. DOI: 10.1039/C7FD00225D

[124] Tomaschun G, Dononelli W, Li Y, Bäumer M, Klüner T, Moskaleva L. Oxidative dehydrogenation of methanol on the Au(310) surface: The role of surface morphology from a DFT modeling study (submitted)

[125] Chang C-R, Yang X-F, Long B, Li J. A water-promoted mechanism of alcohol oxidation on a Au(111) surface: Understanding the catalytic behavior of bulk gold. ACS Catalysis. 2013;**3**(8):1693-1699. DOI: 10.1021/cs400344r

[126] Ojeda M, Zhan B-Z, Iglesia E. Mechanistic interpretation of CO oxidation turnover rates on supported Au clusters. Journal of Catalysis. 2012;**285**(1):92-102. DOI: 10.1016/j. jcat.2011.09.015

[127] Déronzier T, Morfin F, Massin L, Lomello M, Rousset J-L. Pure nanoporous gold powder: Synthesis and catalytic properties. Chemistry of Materials. 2011;**23**(24):5287-5289. DOI: 10.1021/cm202105k

[128] Déronzier T, Morfin F, Lomello M, Rousset J-L. Catalysis on nanoporous gold-silver systems: Synergistic effects toward oxidation reactions and influence of the surface composition. Journal of Catalysis. 2014;**311**:221-229. DOI: 10.1016/j.jcat.2013.12.001

[129] Graf M, Roschning B, Weissmüller J. Nanoporous gold by alloy corrosion: Method-structure-property relationships. Journal of the Electrochemical Society. 2017;**164**(4): C194-C200. DOI: 10.1149/2.1681704jes

[130] Nørskov JK, Bligaard T, Logadottir A, et al. Trends in the exchange current for hydrogen evolution. Journal of the Electrochemical Society. 2005;**152**(3):J23. DOI: 10.1149/1.1856988

[131] Parsons R. Volcano curves in electrochemistry. In: Catalysis in Electrochemistry. Hoboken, New Jersey, United States of America: John Wiley & Sons, Inc.; 2011. pp. 1-15

[132] Kibler LA, El-Aziz AM, Hoyer R, Kolb DM. Tuning reaction rates by lateral strain in a palladium monolayer. Angewandte Chemie, International Edition. 2005;**44**(14):2080-2084. DOI: 10.1002/anie.200462127

[133] Hammer B, Nørskov JK. Electronic factors determining the reactivity of metal surfaces. Surface Science. 1995;**343**(3):211-220. DOI: 10.1016/0039-6028(96)80007-0

[134] Ruban A, Hammer B, Stoltze P, Skriver H, Nørskov J. Surface electronic structure and reactivity of transition and noble metals1Communication presented at the First Francqui Colloquium, Brussels, 19–20 February 1996.1. Journal of Molecular Catalysis A: Chemical. 1997;**115**(3):421-429. DOI: 10.1016/S1381-1169(96)00348-2

[135] Weissmüller J, Viswanath RN, Kibler LA, Kolb DM. Impact of surface mechanics on the reactivity of electrodes. Physical Chemistry Chemical Physics. 2011;**13**(6):2114-2117. DOI: 10.1039/c0cp01742f

[136] Gokhshtein AY. Investigation of surface tension of solid electrodes at several frequencies simultaneously. Electrochimica Acta. 1970;**15**(1):219-223. DOI: 10.1016/0013-4686(70)90023-X

[137] Gokhshtein AY. The estance method. Russian Chemical Reviews. 1975;**44**(11):921

[138] Umeno Y, Elsässer C, Meyer B, et al. Ab initio study of surface stress response to charging. Europhysics Letters. 2007;**78**(1):13001. DOI: 10.1209/0295-5075/78/13001

[139] Smetanin M. Mechanics of electrified interfaces in diluted electrolytes. Saarländische Universitäts- und Landesbibliothek. 2010. https://publikationen.sulb.uni-saarland.de/handle/20.500.11880/25689

[140] Haiss W, Nichols RJ, Sass JK, Charle KP. Linear correlation between surface stress and surface charge in anion adsorption on Au(111). Journal of Electroanalytical Chemistry. 1998;**452**(2):199-202. DOI: 10.1016/S0022-0728(98)00137-5

[141] Viswanath RN, Kramer D, Weissmüller J. Variation of the surface stress−charge coefficient of platinum with electrolyte concentration. Langmuir. 2005;**21**(10):4604-4609. DOI: 10.1021/la0473759

[142] Smetanin M, Viswanath RN, Kramer D, et al. Surface stress-charge response of a (111)-textured gold electrode under conditions of weak ion adsorption. Langmuir. 2008;**24**(16):8561-8567. DOI: 10.1021/la704067z

[143] Smetanin M, Kramer D, Mohanan S, Herr U, Weissmüller J. Response of the potential of a gold electrode to elastic strain. Physical Chemistry Chemical Physics. 2009;**11**(40):9008-9012. DOI: 10.1039/b913448d

[144] Trasatti S. Work function, electronegativity, and electrochemical behaviour of metals: II. Potentials of zero charge and "electrochemical" work functions. Journal of Electroanalytical Chemistry and Interfacial Electrochemistry. 1971;**33**(2):351-378. DOI: 10.1016/S0022-0728(71)80123-7

[145] Rath DL, Kolb DM. Continuous work function monitoring for electrode emersion. Surface Science. 1981;**109**(3):641-647. DOI: 10.1016/0039-6028(81)90432-5

[146] Albina J-M, Elsässer C, Weissmüller J, Gumbsch P, Umeno Y. Ab initio investigation of surface stress response to charging of transition and noble metals. Physical Review B. 2012;**85**(12):959. DOI: 10.1103/PhysRevB.85.125118

[147] Murnaghan FD.The compressibility of media under extreme pressures. Proceedings of the National Academy of Sciences of the United States. 1944;**30**(9):244-247

[148] Hoppe S, Müller S. Electromechanical coupling at Ag-Au surfaces via first principles: Influence of alloy composition and surface segregation (in preparation)

[149] Hoppe S, Müller S. Journal of Applied Physics. 2017;**122**:235-303